Laser Spectroscopy sensor for measurements of trace gaseous sulfur dioxide (SO_2)

by

Anand Matta

Submitted in Partial Fulfillment of the Requirements
for the Degree of

Master of Chemistry

in the

Chemistry

Program

YOUNGSTOWN STATE UNIVERSITY

December, 2008

Laser Spectroscopy sensor for measurements of trace gaseous sulfur dioxide (SO_2)

Anand Matta

I hereby release this thesis to the public. I understand that this thesis will be made available from the OhioLINK ETD Center and the Maag Library Circulation Desk for public access. I also authorize the University or other individuals to make copies of this thesis as needed for scholarly research.

Signature:

_____

Anand Matta, Student Date

Approvals:

_____

Dr. Josef B. Simeonsson, Thesis Advisor Date

_____

Dr. Daryl W. Mincey, Committee Member Date

_____

Dr. Peter Norris, Committee Member Date

_____

Peter J. Kasvinsky, Dean of School of Graduate Studies & Research Date

Abstract:

Laser Induced Fluorescence (LIF) using non tunable laser sources is a method which has been studied for the measurement of atmospheric sulfur dioxide (SO_2). As this approach is direct, there is no need of sample collection or sample concentration and the air sample can be used directly for analysis. In the approach used in these studies, a Nd:YAG laser operating at 266 nm, which is the fourth harmonic of this non-tunable laser, is used as an excitation source. Other wavelengths of excitation at 199 nm, 217 nm and 223 nm can also be used and are produced by Stimulated Raman Scattering (SRS) of 266 nm and 355 nm radiation in compressed hydrogen gas. Studies of the analytical capability of these LIF approaches have been performed at different laser wavelengths. Studies of the fluorescence spectrum signal power dependence, linearity and sensitivity have been performed. The best results have been obtained using excitation at 223 nm resulting in a limit of detection of 0.01 ppm. With further development, it is expected that the LIF approach may be able to perform fast, sensitive measurements of SO_2 in the open environment while avoiding many of the interferences that occur in the conventional methods for SO_2 measurements.

ACKNOWLEDGMENTS

Any acknowledgment of my success must begin by thanking my Lord Almighty to whom I dedicate this work. Without his favor strength and blessings I wouldn't have been able to complete this thesis.

I am greatly indebted to my thesis advisor Dr. Josef B. Simeonsson who made this thesis possible and guided me the whole time in the research. I thank him for the personal and scientific growth, as well as for the training, support, advice and patience.

I would also like to thank my committee members, Dr. Daryl W. Mincey and Dr. Peter Norris for their valuable advices and encouragement. I take this opportunity to thank the chemistry department, Youngstown State University and graduate school for its funding. Very special thanks to all my friends at YSU especially in the chemistry department.

Last but not the least I want to thank my father, mother, brother, sister, grandfather and grandmother who supported me and loved me in all my thick and thin times. I will always be thankful to them for having faith in me and never letting me down.

LIST OF CONTENTS

TITLE PAGE I

SIGNATURE PAGE II

ABSTRACT III

ACKNOWLEDGMENTS IV

LIST OF TABLES VII

LIST OF FIGURES VIII

LIST OF SYMBOLS AND ABBREVIATIONS XI

1. INTRODUCTION 1

    a. BACKGROUND OF SO_2 2

    b. GOAL OF THE PROJECT 3

    c. STATE OF THE ART FOR SO_2 MEASUREMENT 3

    d. LASERS 5

    e. LASER INDUCED FLUORESCENCE 5

    f. UV SPECTROSCOPY OF SO_2 8

    g. PERMEATION TUBE DEVICES 9

    h. SAMPLE CELL 10

    i. MOMOCHROMATOR 12

    j. PMT (PHOTOMULTIPLIER TUBE) 13

    k. STIMULATED RAMAN SCATTERING 14

    l. OPTICAL FILTERS 16

    m. LONG PASS FILTERS 16

n. SHORT PASS FILTERS 16

o. BAND PASS FILTERS 16

p. NEUTRAL DENSITY FILTERS 16

q. ABSORPTION FILTERS 16

2. EXPERIMENTAL 18

a. INSTRUMENTATION 19

b. STUDIES OF SO_2 20

3. RESULTS AND DISCUSSION 24

a. SPECTRUM OF SO_2 WITH 266 nm LASER 25

b. POWER DEPENDENCE 26

c. CALIBRATION CURVE STUDIES OF SO_2 USING 266 nm LASER 27

d. OUTPUT SCANS OF 266 nm FROM THE RAMAN CONVERTOR 28

e. OUTPUT SCANS OF 355 nm FROM THE RAMAN CONVERTOR 29

f. SPECTRUM OF SO_2 WITH 223 nm LASER 31

g. RELATIVE INTENSITIES 34

h. TRIALS WITH 199 nm AND 217 nm LASER 36

i. CALIBRATION CURVE STUDIES OF 223 nm LASER 37

j. COMPARISON OF RESULTS OF 266 nm AND 223 nm 44

k. COMPARISON OF SIGNAL AND BACKGROUND FOR 266 nm AND 223 nm 44

l. INTERFERENCE STUDIES OF FORMALDEHYDE (HCHO) 45

m. OTHER INTERFERENCES 46

n. COMPARISON OF LOD WITH OTHER WORKS 48

o. CONCLUSIONS 49

p. FURTHER STUDIES 49

4. REFERENCES 51

LIST OF TABLES

TABLE: (1) SCANNING PARAMETERS FOR THE FLUORESCENCE OF 266 nm LASER EXCITATION 21

TABLE: (2) CALIBRATION CURVE PARAMETERS FOR 266 nm LASER EXCITATION 22

TABLE: (3) OUTPUTS OF 226 nm LASER THROUGH RAMAN CONVERTOR 33

TABLE: (4) OUTPUTS OF 355 nm LASER THROUGH RAMAN CONVERTOR 33

TABLE: (5) RELATIVE STIMULATED RAMAN SCATTERING INTENSITIES OF 266 nm LASER RADIATION 34

TABLE: (6) RELATIVE STIMULATED RAMAN SCATTERING INTENSITIES OF 355 nm LASER RADIATION 35

TABLE: (7) COMPARISON OF SIGNAL AND BACKGROUND FOR 266 nm AND 223 nm LASER EXCITATION 44

TABLE: (8) COMPARISON OF LIMIT OF DETECTION OF THIS WORK WITH OTHER STUDIES 48

LIST OF FIGURES

FIGURE: (1) SCHEMATIC DIAGRAM OF A LASER 5

FIGURE: (2) PRINCIPLE OF FLUORESCENCE 7

FIGURE: (3) SCHEMATIC DIAGRAM OF THE INSTRUMENTATION 8

FIGURE: (4) PICTURE OF THE CLOSED SAMPLE CELL 11

FIGURE: (5) PICTURE OF THE OPEN SAMPLE CELL 12

FIGURE: (6) DIAGRAM OF A GRATING IN THE MONOCHROMATOR 13

FIGURE: (7) DIAGRAM OF A PHOTOMULTIPLIER TUBE (PMT) 14

FIGURE: (8) PRINCIPLE OF STIMULATED RAMAN SCATTERING 15

FIGURE: (9) BLOCK DIAGRAM OF THE INSTRUMENTATION 19

FIGURE: (10) BLOCK DIAGRAM OF THE INSTRUMENT FOR POWER DEPENDENCE 20

FIGURE: (11) BLOCK DIAGRAM OF THE INSTRUMENT WITH THE RAMAN CONVERTOR 23

FIGURE: (12) SPECTRUM OF SO_2 FROM 275 nm - 400 nm WITH TOLUENE FILTER 25

FIGURE: (13) POWER DEPENDENCE OF SO_2 FLUORESCENCE WITH 266 nm LASER EXCITATION AND FLUORESCENCE WAVELENGTH OF 360 nm 26

FIGURE: (14) ABSORPTION SPECTRUM OF TOLUENE FILTER 27

FIGURE: (15) CALIBRATION CURVE OF SO_2 FLUORESCENCE WITH 266 nm LASER EXCITATION AT DIFFERENT SLIT WIDTHS 28

FIGURE: (16) CALIBRATION CURVE OF SO_2 FLUORESCENCE WITH 266 nm LASER EXCITATION AND MONOCHROMATOR @ 325 29

FIGURE: (17) SCAN OF THE OUTPUTS OF 266 nm LASER THROUGH RAMAN CONVERTOR 30

FIGURE: (18) SCAN OF THE OUTPUTS OF 355 nm LASER THROUGH RAMAN CONVERTOR 30

FIGURE: (19) SPECTRUM OF SO_2 FLUORESCENCE WITH 223 nm LASER EXCITATION 32

FIGURE: (20) POWER DEPENDENCE OF SO_2 FLUORESCENCE WITH 223 nm LASER EXCITATION, CLOSED SAMPLE CELL AND MONOCHROMATOR 37

FIGURE: (21) CALIBRATION CURVE OF SO_2 FLUORESCENCE WITH 223 nm LASER EXCITATION, CLOSED SAMPLE CELL AND MONOCHROMATOR 38

FIGURE: (22) ABSORPTION SPECTRUM OF THE 334 nm BAND PASS FILTER 39

FIGURE: (23) CALIBRATION CURVE OF SO_2 FLUORESCENCE WITH 223 nm LASER EXCITIAION, CLOSED SAMPLE CELL, CYLINDRICAL FOCUSING LENS AND PMT/FILTER 39

FIGURE: (24) CALIBRATION OF SO_2 FLUORESCENCE WITH 223 nm LASER EXCITATION, T-CELL AND @ DIFFERENT TEMPERATURES 40

FIGURE: (25) CALIBRATION CURVE OF SO_2 FLUORESCENCE WITH 223 nm LASER EXCITATION, T-CELL AND @ DIFFERENT SLIT WIDTHS 41

FIGURE: (26) CALIBRATION CURVE OF SO_2 @ TEMP-40 ^{0}C, WITH PMT FILTER, T-CELL AND FOCUSING LENS 42

FIGURE: (27) POWER DEPENDENCE OF SO_2 FLUORESCENCE WITH 223 nm LASER EXCITATION, T-CELL AND MONOCHROMATOR 43

FIGURE: (28) POWER DEPENDENCE OF SO_2 FLUORESCENCE WITH 223 nm LASER EXCITATION, T-CELL AND PMT/FILTER 43

FIGURE: (29) SPECTRUM OF HCHO FLUORESCENCE WITH 223 nm LASER EXCITATION FOR INTERFERENCE STUDIES 46

FIGURE: (30) CALIBRATION CURVE OF HCHO FLUORESCENCE WITH 223 nm LASER EXCITATION FOR INTERFERENCE STUDIES 47

LIST OF SYMBOLS AND ABBREVIATIONS

% ……..…..percentage

ν…….Nu

Δ……Delta

µg…….Microgram

µm……...Micrometer

µs……...……Microsecond

a.u.…….…..……arbitrary units

Å…….....……..Angstroms

A……..Absorbance

A…….Area

APIMS……...……..…Atmospheric pressure ionization mass spectrometry

c……...Concentration

CCD……...Charge coupled device

Cd……...Cadmium

cm…….……..……..Centimeter

D……...……Optical Density

DOAS……...…….……..Differential optical absorption spectrometry

eV……..……Electron volt

FEP……...Fluorinated ethylene propylene

GC……Gas Chromatography

hν……photon energy

H_2……...Hydrogen

H_2O……...Water

HCHO…….Formaldehyde

HCl……Hydrochloric acid

HPLC…….. High performance liquid chromatography

Hz……..…….……Hertz

K……..……Kelvin

kg…….……...Kilogram

kW……Kilowatt

L……Liter

l……Length

LASER…… Light Amplification by Stimulated Emission of Radiation

LIF……Laser Induced Fluorescence

LOD……Limit of detection

LOQ……Limit of quantification

m/v……mass per volume

M……Molar

m……Meter

MHz……Mega Hertz

min……minute

mJ……Millijoules

mL……milliliter

mm……Millimeter

MS……Mass Spectrometry

mV……Millivolts

Nd:YAG……Neodymium-doped yttrium aluminum garnet

ND……Neutral Density

ng……Nanogram

nm……Nanometer

NO_2……Nitrogen Dioxide

ns……Nanosecond

O……Oxygen

^0C……Degree Celsius

PDA…… Photodiode array

PMT……Photomultiplier tube

ppb……Parts per billion

ppm……Parts per million

ppt……Parts per trillion

psi……Pound per Square Inch

r.p.m…… rotation per minute

RF……..……..…..……Radiofrequency

RSD……Relative standard deviation

SO_2……...……..Sulfur Dioxide

SRS……...…….……...…Stimulated Raman Scattering

TFE…….Tetrafluoroethylene

US-EPA……United States Environmental Protection Agency

UV……..….Ultra Violet

v/v……..volume per volume

V…….……..…….Volts

Zn……..……..Zinc

α……..Alfa

λ……..Wavelength

σ……..Standard Deviation

1. INTRODUCTION

a. Background of SO_2:

Sulfur dioxide (SO_2) is a colorless, reactive gas with a strong odor that dissolves in water and water vapor. It is produced as a result of the combustion of fossil fuels such as coal and oil and is also a byproduct of the smelting of iron ore. Sulfur dioxide is also produced naturally from volcanoes, oceans, biological decay and forest fires. The two major man made sources of SO_2 are burning of coal and burning of fossil fuel.[1, 2] Sulfur dioxide and the pollutants formed from SO_2, such as sulfate particles, can be transported over long distances and deposited far from the source. As a result, the pollution impacts are not limited to areas where it is emitted. In air, SO_2 mixes with water vapor and produces sulfuric acid which leads to acid precipitation, resulting in soil acidification, and the erosion of building materials.

In humans, long term exposures to high levels of SO_2 gas and related particles cause respiratory illnesses and can aggravate existing heart diseases. People with asthma who are active outdoors are most vulnerable to the health effects of SO_2.[3] When exposed to SO_2, these people show symptoms such as wheezing, chest tightness, and shortness of breath, where the symptoms increase with increase in the concentration of SO_2. At high concentrations, even people without asthma can show similar symptoms. Sulfur dioxide reacts with other chemicals in the air to form tiny sulfate particles. When these are inhaled, they gather in the lungs and are associated with increased respiratory symptoms and diseases. The threshold limit for humans over an 8 hour work day or 40 hour work week is 2 ppm.[3] Sulfur dioxide forms sulfuric acid when it comes in contact with moist surfaces such as eyes, mucous membranes, and skin. This sulfuric acid decreases the body's ability to clear particles in the pulmonary tube, which is a major protective

mechanism of the lungs. A concentration of 4 ppm can be detected by its odor, 8 – 12 ppm will cause coughing and 20 ppm will cause eye irritation.[3]

The main environmental effect of SO_2 is the production of acid rain. Acid rain damages forests and crops, changes the makeup of soil, and makes lakes and streams acidic and unsuitable for fish. The soil acidification can also lead to forest decline. Continued exposure over a long time changes the natural variety of plants and animals in an ecosystem. Sulfur dioxide also accelerates the decay of building material and paints, including monuments, statues, and sculptures.

Apart from its harmful effects, SO_2 also has some uses. It is used as a preservative in dry fruits[4] and also in the manufacture of wine. In the preparation of wine, it is used as an anti-microbial agent, as an anti-oxidant and as a destabilizer of disulfide bridges in enzymes which helps to prevent enzymatic browning.[5] Sulfur dioxide acts as an anti-microbial agent and it acts as an anti-oxidant due to its ability to remove hydrogen peroxide and molecular oxygen.[5]

b. <u>Goal of the project</u>:

The main purpose of this project is to investigate a laser induced fluorescence approach for the trace detection of SO_2 in the atmosphere that is direct and uses a non-tunable laser. It is anticipated that this approach may have advantages over conventional methods for measuring SO_2.

c. <u>State of the art for SO_2 measurement</u>:

Due to the harmful effects, SO_2 needs to be regulated and monitored on a continual basis. The monitoring of SO_2 in the vapor phase has been performed using different analytical techniques. The reference methods are the West-Gaeke method[1] and

flame photometric method.[6] In the first method, the formation of a red-violet color is observed when SO_2 reacts with pararosaniline, hydrochloric acid, and formaldehyde. One of the interferences in this method is NO_2. The detection limit is reported to be about 10 ppb.[6]

The flame photometric method is based on the measurement of sulfur emission bands that occur when SO_2 is burned in a hydrogen-air flame. A narrow band optical filter is used which has a maximum transmission at 3940 Å.

Fluorescence spectroscopy is also used to monitor SO_2 where the intensity of the fluorescence excited by a Cd lamp at 228 nm. Due to the decrease in fluorescence caused by H_2O, Zn lamp excitation at 213 nm has also been used to excite SO_2 fluorescence,[7, 8] due to which the detection limit is improved to the ppb range. It has been proposed that the limit of detection (LOD) can be further improved to the ppb range with the use of a more intense light source such as a laser source.[8]

There are also other measurement methods such as aqueous chemiluminescence,[9] pulsed fluorescence,[10] isotope dilution-gas chromatography mass spectrometyr,[11] mist chamber ion chromatography,[12] diffusion denuder sulfur chemiluminescence detector,[13] high performance liquid chromatography with fluorescence detection,[14] carbonate filter ion chromatography,[15] atmospheric pressure ionization mass spectrometry (APIMS),[16] and differential optical absorption spectrometry (DOAS).[17] Laser induced fluorescence (LIF) has been shown previously to provide detection limits to the pptv[18] level. Using a tunable laser source, the LIF method has recently been developed to get improved detection limits down to 5 pptv with a signal to noise ratio of 2.[19]

d. Lasers:

A laser [figure (1)] is generally based on an optical resonator which is a closed cavity with an arrangement of optical components where light reflects within the closed path. In this optical resonator, the gain medium is present, which is used to amplify the light by a stimulated emission process. The gain medium must be supplied with external energy such as light or electric current. This energy is converted to laser radiation by the stimulated emission process. There are different kinds of lasers such as semiconductor lasers, solid state lasers, fiber lasers and gas lasers.

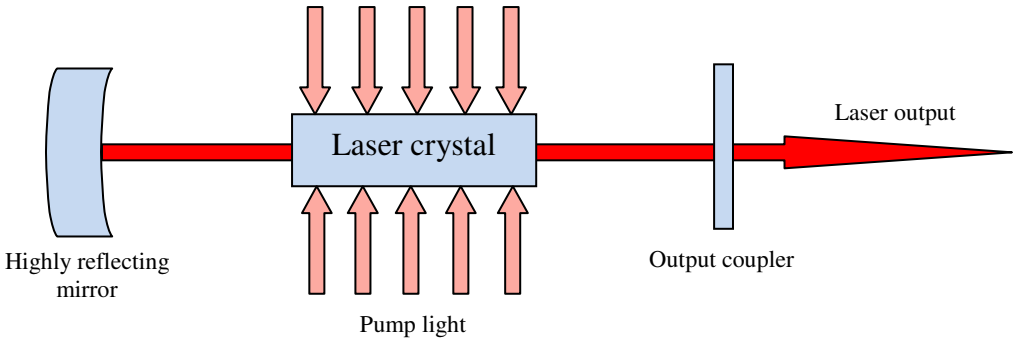

Figure: (1) Schematic diagram of a laser

A Nd:YAG laser has been used in these studies for the LIF of SO_2. The term Nd:YAG was given to it due to the type of crystal that is used. The crystal is neodymium-doped yttrium aluminum garnet (Nd:YAG). This laser emits at a wavelength of 1064 nm, which is called the fundamental wavelength. Other wavelengths such as 532 nm, 355 nm and 266 nm can be generated by nonlinear conversion processes.

e. Laser Induced Fluorescence:

Laser Induced Fluorescence (LIF) is the fluorescence emission produced from an atom or molecule when a laser is used as an excitation source. Fluorescence is a two step

process in which absorption and relaxation occurs and fluorescence emission is given out during the relaxation process. Absorption occurs when light is absorbed by a molecule or an atom. The particle gains energy and goes to an excited state or higher energy state. This process of absorption can be explained by the Beer-Lambert law.[20] This law gives the relation between the absorption and the concentration of the absorption species. It can be written as

$$A = a(\lambda) * b * c \quad (4)$$

Where A = measured absorbance

$a(\lambda)$ = wavelength-dependent absorptivity coefficient

b = path length

c = analyte concentration

The excited molecules or atoms relax to a lower energy level by giving out energy in the form of radiation, which is also called emission or luminescence. In the case of fluorescence, the molecule may not return to the original ground state, in which case the emitted light is different in wavelength from the wavelength of absorption. The fluorescence method is widely used for the detection and monitoring of gas-phase concentrations in the atmosphere, flames, and plasmas. This method can be used in the detection of trace amounts of pollutants in the air as well.

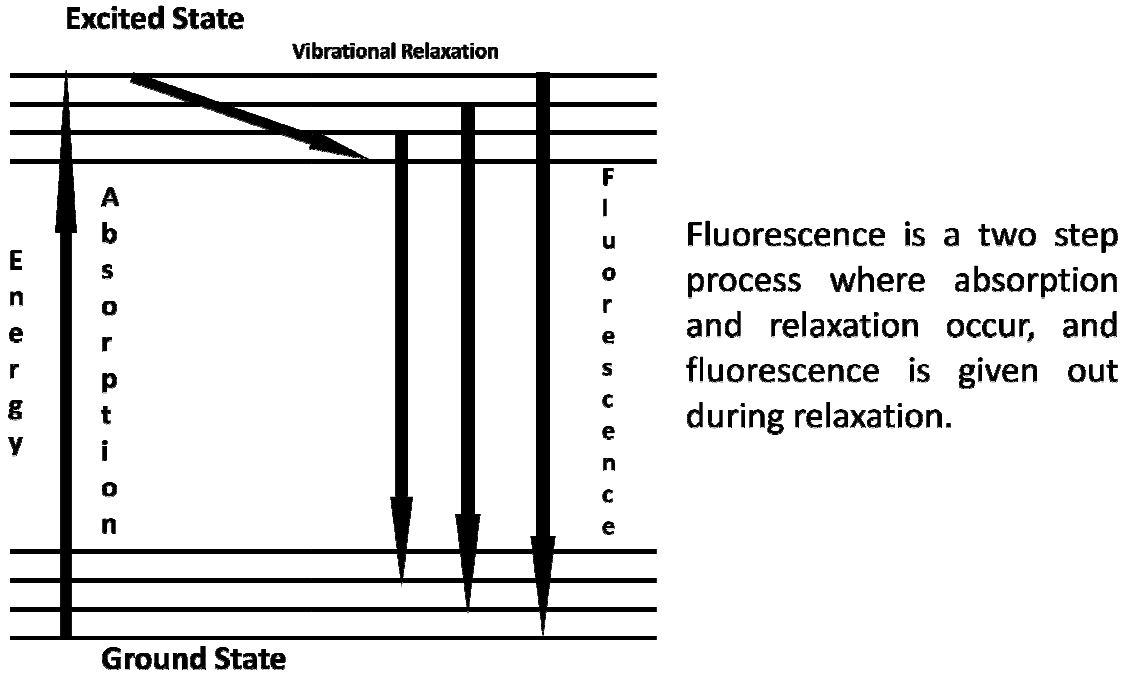

Figure: (2) Principle of Fluorescence

In the case of LIF, a laser is used as a light source for the excitation of the analyte molecules. The analyte molecules absorb energy and are excited to higher energy levels and then emit fluorescence where the fluorescence intensity is directly proportional to the amount of analyte present. The analyte under study, SO_2, is being quantified using LIF techniques. Laser light of 266 nm which is the fourth harmonic of the Nd:YAG laser, has been used as one of the light sources. The fluorescence given out by SO_2 ranges between 275 to 400 nm.[19] This fluorescence is detected with the help of a monochromator and detector setup. The general experimental setup is in figure (3).

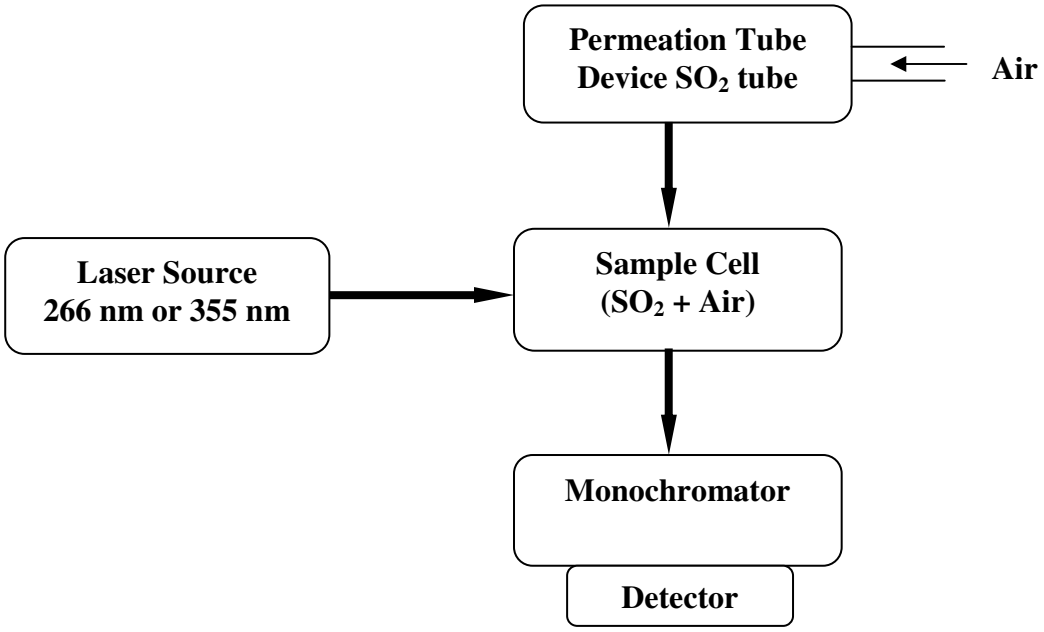

Figure: (3) Schematic diagram of the instrumentation

f. <u>UV Spectroscopy of SO_2</u>:

There are two important absorption systems seen in the UV spectrum of SO_2. One system is from 170 – 230 nm which is a densely packed system of lines assigned to the $\tilde{C}\ ^1B_2 - \tilde{X}\ ^1A_1$ electronic transition.[21] The second region is of a relatively weaker system ranging from approximately 240 – 338 nm and is mainly due to the $\tilde{B}\ ^1B_1 - \tilde{X}\ ^1A_1$ transition.[21] The UV spectral region $\tilde{A}\ ^1B_1 - \tilde{X}\ ^1A_1$ is considered to be good candidate to monitor the fluorescence of SO_2.[22] The fourth harmonic of the Nd:YAG laser can be used directly as an excitation source.[23] For the absorption spectral range of 170 – 230 nm, the excitation wavelengths can be generated using the third harmonic of the Nd:YAG laser. This laser radiation is passed through a Raman cell containing Hydrogen gas which gives out different frequencies due to Stimulated Raman Scattering (SRS) processes. The SRS approach is discussed in detail in the following chapters.

In the single photon LIF study of SO_2 by Bradshaw et al.[18] a non tunable Nd:YAG laser with fundamental at 1064 nm was used and two different dyes for the harmonic generation 226 nm and 222 nm. All the measurements were performed under atmospheric conditions, that is at atmospheric pressure and temperature. A cooled *KD*P* frequency mixing crystal was used and the fluorescence was collected at $\sim$15 nm band width with the center being at $\sim$260 nm. The diluent gas was scrubbed before mixing with the standard SO_2 to remove any impurities and H_2O. The LOD obtained for SO_2 was 4 pptv with an integration time of 20 min and laser excitation at 222.9 nm with laser energy 1 mJ.

The study on LIF of SO_2 by Yutalka Matsumi et al.[19] used a tunable-band optical parametric oscillator (OPO) pumped by the third harmonic of a Nd:YAG laser as an excitation source. The laser wavelength was 220.6 nm. A two wavelength measurement technique was (220.6 nm and 220.2 nm) which avoids the interferences of other species that give out fluorescence. A band pass optical filter was used to isolate the emitted fluorescence of SO_2 from 240 nm – 420 nm. Light baffles were used to prevent the scattering of the light from the windows of the sample cell. The LOD was 5 pptv with an integration time of 60 sec. and the laser pulse energy was 1 mJ.

g. <u>Permeation tube devices</u>:

The constant supply of SO_2 used for calibration in these studies is produced by the use of a permeation tube device. This is a temperature controlled device which produces analyte vapor at a constant rate at a constant temperature. The rate of vapor production increases with the temperature of the device. Permeation tubes are small tubes filled with pure analyte compound. These tubes are typically made of tetrafluoroethylene (TFE) or

fluorinated ethylene propylene (FEP) Teflon, as these materials are durable and low in reactivity. The volatile liquid of the pure compound is sealed in a cylindrical tube. The permeation process starts when the temperature is increased. As volatile liquid turns to vapor, it diffuses through the polymer wall of the tube and mixes with the air flow on the outside of the tube. The Fick's law of diffusion describes the flow of analyte gas from the tube.[24] This occurs due to the difference in the partial pressure between the inner and outer tube walls. It is suggested as a common rule of thumb that every $1^{o}C$ increase produces a 10% change in the permeation rate.[24]

$$q_d = (p_\delta A \Delta P)/L \quad (5)$$

$$p_\delta = D\ S \quad (6)$$

Where q_d – is the amount of sample material that passes through the permeation material.

A – is the area of the material

ΔP – is the pressure difference across the polymer

L – is the thickness of the polymer

p_δ – is the fluid permeability constant

D – is the diffusion coefficient

S – is solubility constant of the fluid in the polymer.

From the equations (5) and (6), it is seen that the two important factors that affect the release of gas from the tube are (1) the difference in pressure across the wall of the permeation tube and (2) the solubility of the permeation fluid in the polymer.[25]

h. <u>Sample cell</u>:

One sample cell used in these studies is made of stainless steel (Figure 4) with quartz windows on three sides. These windows allow the entry and exit of the laser

radiation and also the exit of the fluorescence emission, which goes to a monochromator and detector setup. This sample cell is fitted with an inlet for the sample gas and an outlet to vent the chamber. The windows are made of quartz to allow transmission of ultraviolet wavelength.

This cell was replaced in some studies with a simple "T" shaped cell (Figure 5), as the stainless steel cell can have a high background due to the laser beam reflecting from the windows. The T – cell is made of quartz and is open at both ends which helps to reduce the reflection and scattering background. The open cell has an inlet for gas and the gas escapes from the open ends of the cell.

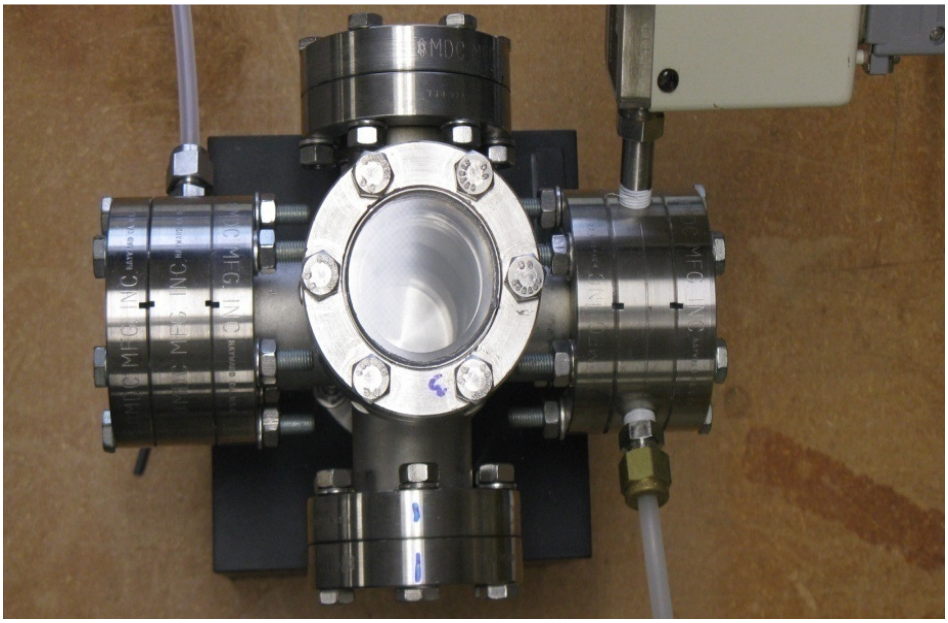

Figure: (4) Picture of the closed sample cell

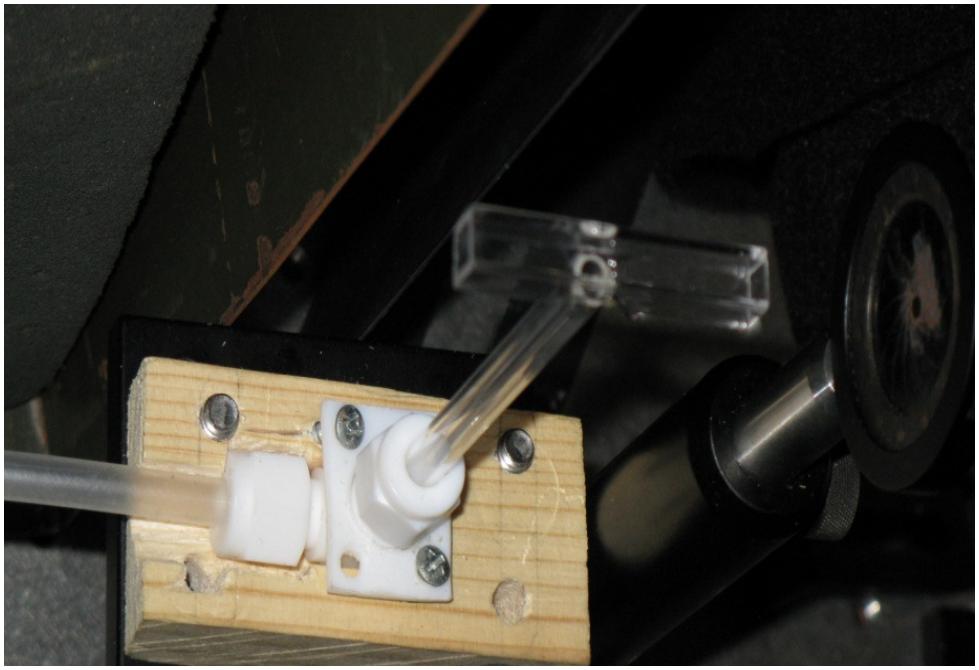

Figure: (5) Picture of the open sample cell

i. <u>Monochromator</u>:

The fluorescence emission produced in the sample cell was directed to a monochromator. A monochromator is an optical device which helps to separate a desired wavelength from a range of wavelengths. The monochromator has two slits, one for entry of the light and one for the exit. These help to control the amount of light that enters the instrument and detector. The transmitted light is directed to a mirror which reflects the light onto a grating. A grating is a dispersion element in the monochromator that is used to disperse the incoming parallel light that contains different wavelengths into independent rays of light that are no longer parallel to each other. After striking the grating, the parallel beam of light is reflected at different angles depending on the wavelength. Figure (6) shows a schematic diagram of a grating. The desired wavelength

is selected by changing the angle of the grating. The wavelength that is chosen is sent out through the exit slit while the rest of the light is absorbed inside the monochromator.

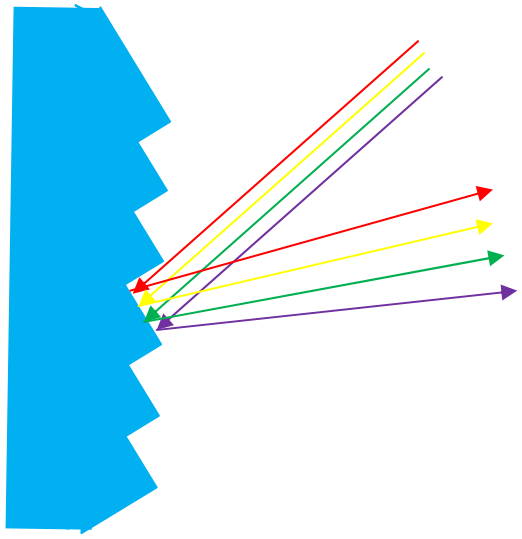

Figure: (6) Diagram of a grating in the monochromator

j. <u>PMT (Photomultiplier Tube)</u>:

Light that is transmitted out of the monochromator is detected and quantified using a PMT (Photomultiplier tube) (Figure 7). A PMT is made up of a photocathode, a series of dynodes, and an anode which are mounted in a vacuum glass tube. When a photon hits the photocathode, it produces an electron due to the photoelectric effect. This electron is then directed to the dynodes for electron amplification. There are several dynodes and each one is maintained at a higher positive voltage than the previous one. When the photoelectron hits the first dynode it gives out more electrons which are all sent towards the second dynode. As each electron travels through the series of the dynodes, the electrons are multiplied by the same process. These electrons reach the anode which

gives out an electrical impulse that is related to the incident photon. These signals are used to measure the amount of light emissions.

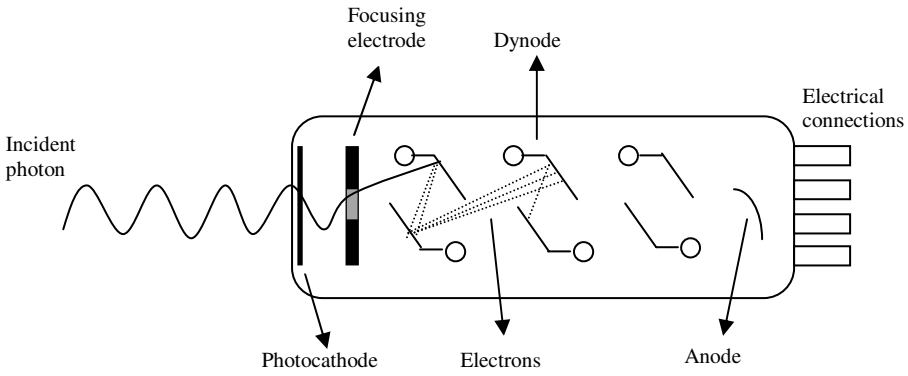

Figure: (7) Diagram of a Photomultiplier Tube (PMT)

k. <u>Stimulated Raman Scattering</u>:

Raman scattering is a process in which inelastic scattering of photons occurs. It is called inelastic scattering due to the fact that the energy of the incident photon is different from the energy of the scattered photon. If the photon transfers the energy to the interacting matter, it is called Stokes Raman scattering. If the photon gains energy from the interacting matter, it is called anti-Stokes Raman scattering. This can be explained using the following diagram [figure (8)].

The molecule is initially at the energy level E_2 when the photon interacts with the molecule exciting it to a higher energy equal to $h\nu_i$. This molecule immediately relaxes back to a different energy level by losing a photon. If the molecule relaxes to E_1, it will lose energy and the photon released will have energy $h\nu_{r1}$. In this case, $h\nu_{r1}$ is more than $h\nu_i$. This is called anti-Stokes Raman scattering. If the molecule relaxes to E_3, it will gain

energy and the photon released will have energy $h\nu_{r2}$. In this case, $h\nu_{r2}$ will be less than $h\nu_i$. This is called Stokes Raman scattering.

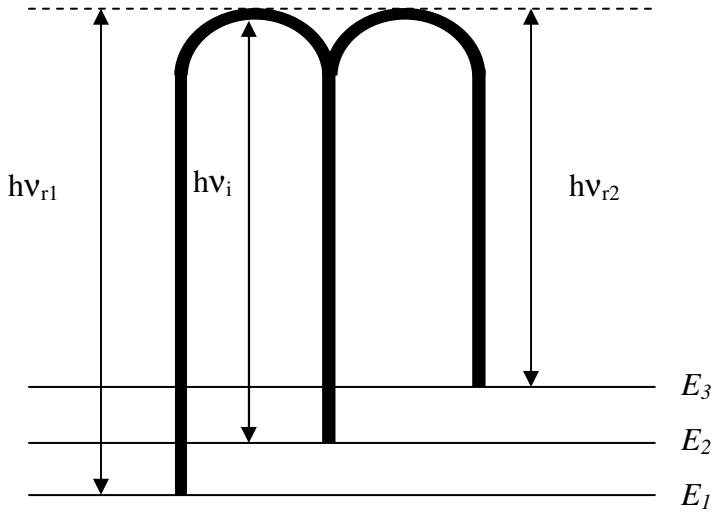

Figure: (8) Principle of Stimulated Raman Scattering

Stimulated Raman scattering is useful in producing different wavelengths from a single wavelength light source. In stimulated Raman Scattering, a pump laser beam interacts with a Raman scattering medium in a four wave mixing process to produce new wavelengths that are separated in energy by multiples of the Raman frequency of the medium. Hydrogen gas is often used as the medium because it has a high conversion efficiency. Several output frequencies are generated when 266 nm and 355 nm radiation are used that range from the ultraviolet to visible wavelength range.[26] The maximum SRS output depends on the pressure of the gas inside the SRS cell, the temperature of the gas and the laser intensity.[25]

l. Optical Filters:

Optical filters are used to block a certain range of wavelengths and at the same time transmit other wavelengths. There are different kinds of filters such as long pass filters, short pass, band pass filters, neutral density filters, and absorption filters that have been used in these studies.

m. Long pass filters: These filters block shorter wavelengths and transmit longer wavelengths above the cut off wavelength.

n. Short pass filter: A short pass filter blocks longer wavelengths and transmit shorter wavelengths below the cut off wavelength.

o. Band pass filter: A band pass filter can be viewed as a combination of a long pass filters and short pass filter that allows only a narrow band of wavelength to be transmitted.

p. Neutral density filters: These filters are used to decrease the intensity of the incoming light. Usually metal films of chromium or nickel on quartz substrates are used. These filters should have constant attenuation over a large spectral range. A neutral density filter with optical density D = 1 has a transmittance T of (10%).[27] D can be determined by the following equation (8).

$$D = \log_{10} (1/T) \quad (8)$$

q. Absorption filters:

These filters block certain ranges of wavelengths and at the same time transmit a different range of wavelengths. These filters are usually colored glass or plastic materials, where the material contains an absorber whose absorption is due to simple or complex ions such as nickel, cobalt, neodymium, or uranium. A quartz cuvette filled with organic

liquids can also be used as high pass absorption filters with cut-off in the UV region. Water solutions of inorganic salts can be used. For example, a mixture of nickel sulphate and cobalt sulphate can used to block the visible region but transmits UV light. Some organic solvents have also been studied for their absorption properties of the UV region.[35] Some of the organic solvents that have been used as filters for the UV region are benzene, toluene, benzonitrile, pyridine, and acetone.[35] Toluene has been used as a solution filter in some of the studies reported here.

2. EXPERIMENTAL

a. <u>Instrumentation</u>:

The overall experimental system includes several components such as a laser source, fluorescence detection system, and a gas generating system (figure: 9). A permeation tube device (Dynacalibrator 230 VICI Metronics) provides a constant flow of SO_2 and air mixtures and the flow rate of the gas is controlled by a flow meter (Cole Parmer # 2B). The gas flows into a 2 inch stainless steel sample flow cell. A Nd: YAG (DCR-IA, Spectra Physics) laser at 266 nm was used as a light source. An oscilloscope (Tektronix TDS 350) was used to monitor the laser energy using an energy meter (Gentec – E/O QEA-25). A monochromator (Acton Research Corporation – Spectra Pro – 275) was used to obtained spectral measurements of the fluorescence emissions. The detector signal was averaged using a boxcar (SR 250. SRS Inc.) and the signal was acquired on a computer using commercial software (SR 272 Data Acquisition Program). The basic setup of the apparatus is shown in the following schematic diagram figure: (9).

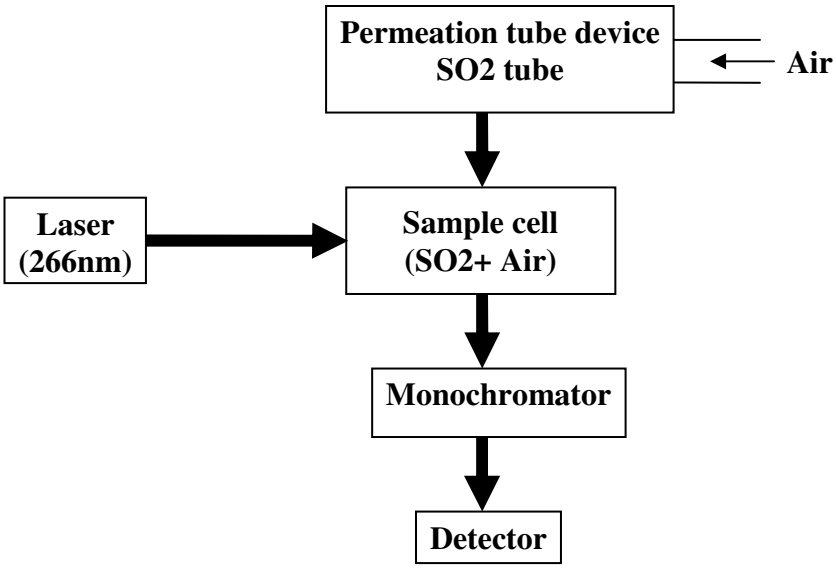

Figure: (9) Block diagram of the instrumentation

b. Studies of SO_2:

For most calibration studies, the SO_2 permeation tube was inserted in the permeation tube device and the temperature was set to 50 ^{0}C. This is the temperature at which the tube is to be maintained to get the maximum flow of SO_2. For fluorescence measurements, the laser was turned on and the 266 nm laser wavelength was generated by adjusting the harmonic generator on the laser system. The laser beam was directed to the sample cell to excite the SO_2. For power dependence studies, the laser intensity was adjusted systematically using a laser attenuator (Newport Research Corp.) Fluorescence emissions were given out by the SO_2 and detected by the monochromator. Further studies were done using this set up (figure: 10).

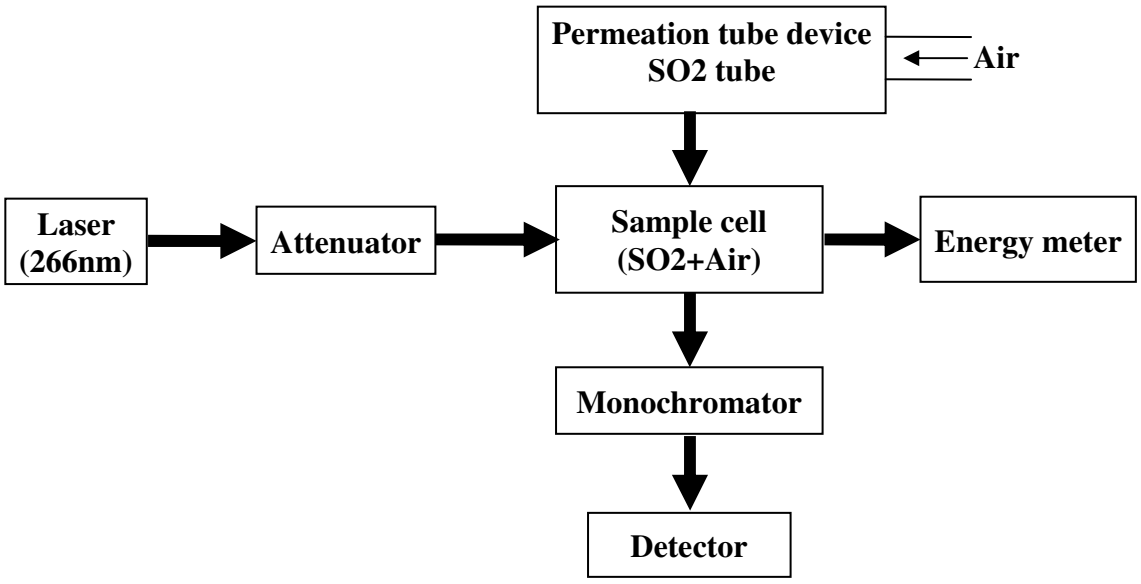

Figure: (10) Block diagram of the instrument for Power Dependence

A flow meter was installed to control the air flow and the concentration of the analyte entering the sample cell. The flow meter dilutes the gas flow from the Dynacalibrator before it reaches the sample cell. The dilutions were made by allowing different amounts of air through the flow meter. The calibration starts from the maximum air flow rates to the minimum air flow rates which correspond to increasing the analyte concentration. It was observed that the higher concentrations in the sample cell take a longer time to clear than the lower concentrations. The signal to noise ratio studies were done by keeping the temperature of the oven constant (50 ^{0}C) and the laser pulse energy at 266 nm was maintained at 4 mJ/pulse. The signal was measured at different energies for the analyte and then the signal of the blank (air only) was taken 16 times. A time gap of at least 10 min was used when changing concentrations to allow the analyte to be removed from the cell.

For spectral studies, fluorescence emissions were taken from 275 nm – 400 nm using different sets of conditions as shown in the following table: (1).

Scan wavelength	**Scan rate**	**Averaging on the box car**	**Energy mJ**	**Slit width**
275 – 400 nm	25 nm / min	30 shots	4 mJ	750
275 – 400 nm	10 nm / min	100 shots	4 mJ	750
275 – 400 nm	10 nm / min	100 shots	1, 2 3, & 4 mJ	750

Table: (1) Scanning parameters for the fluorescence of 266 nm laser excitation

Power dependence studies were performed at different laser energies starting from 0.1 mJ to 8 mJ with an interval of approximately 1 mJ. The temperature was kept constant at 50 ^{0}C, the averaging on the box car was 100 shots and the slit width on the monochromator

was 1000 microns. Calibration curves at different sets of conditions were also performed. The different conditions are given in the following table: (2).

Energy (mJ)	Slit (microns)	Averaging (shots)	Gain mV/V	Filter used	Fluorescence Wavelength (nm)
0.5	1000	100	10	No filter	360
0.5	1000	100	10	Toluene solution filter & ND 1 filter	360
0.5	1000	100	10	Toluene solution filter & ND 1 filter	360
0.5	1000	100	10	Only Toluene solution filter	360
0.5	1000	100	10	Only Toluene solution filter	325
0.5	1000	1000	10	Only Toluene solution filter	325
0.5	1000	1000	10	Only Toluene solution filter	360
0.5	500	1000	10	Only Toluene solution filter	360
0.5	1500	1000	10	Only Toluene solution filter	360
0.5	750	1000	10	Only Toluene solution filter	360
0.5	3000	1000	20	Only Toluene solution filter	360
0.5	1000	1000	10	Toluene solution filter & ND 1 filter	360

Table: (2) Calibration curve parameters for 266 nm laser excitation

Stimulated Raman Scattering of the laser radiation was produced using a Raman Convertor (Light Age Inc. 0.3 m). This is a stainless steel cell with two windows on opposite sides. The cell is filled with hydrogen gas at a pressure of 500 psi. The UV laser at 266 nm or 355 nm was sent through the Raman Convertor which resulted in nine

different output wavelengths due to SRS. The setup of the apparatus is given below figure: (11). Details of experiments performed using SRS generated outputs are discussed in later sections.

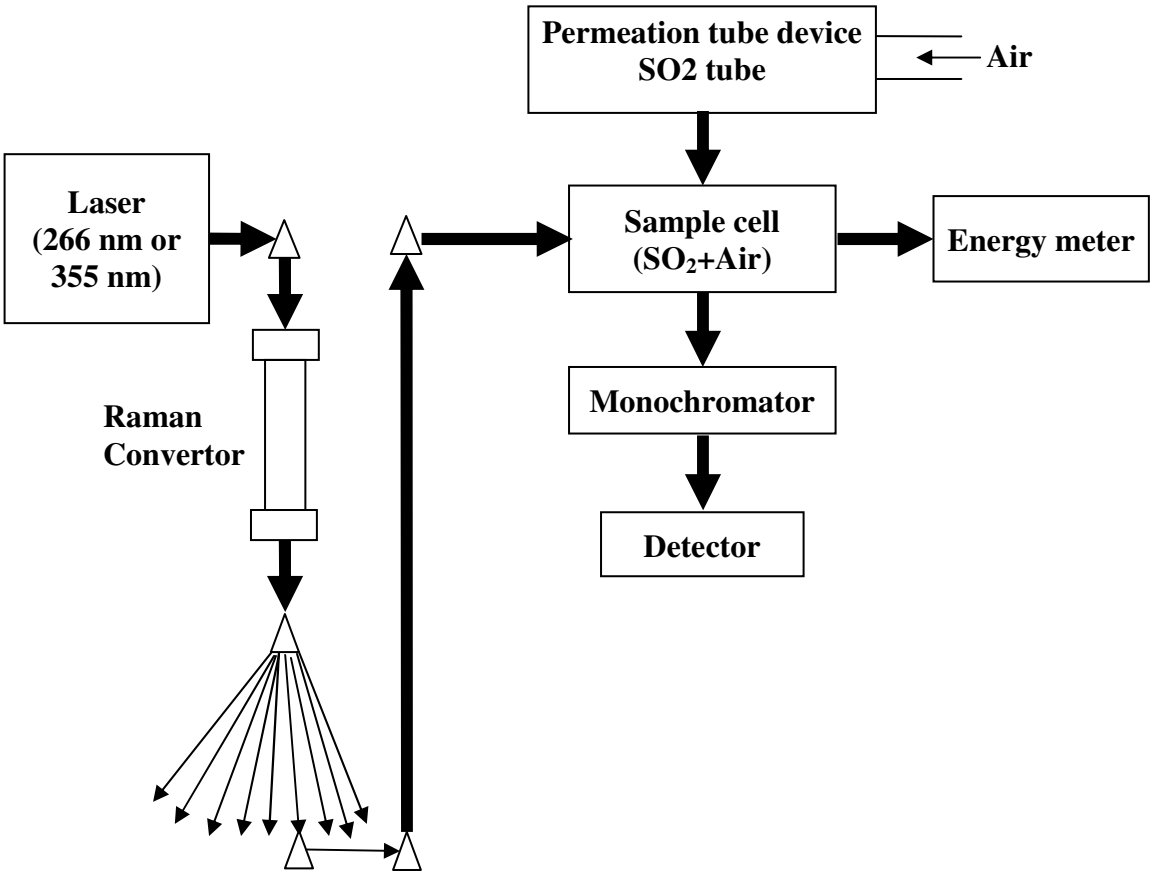

Figure: (11) Block diagram of the instrument with the Raman convertor

3.RESULTS AND DISCUSSION

a. Spectrum of SO_2 with 266 nm laser:

The first studies preformed were to characterize the fluorescence emission of SO_2 when excited at 266 nm. The scan of SO_2 was taken from 275 nm – 400 nm figure: (12) with the laser energy at 3 mJ and the scan rate at 10 nm per min. The fluorescence spectrum of SO_2 following excitation at 266 nm [19] is relatively constant and appears as a continuous band from the excitation wavelength to over 400 nm. An absorption filter (toluene filter) placed at the entrance of the monochromator is used to block any UV light at wavelengths lower than 275 nm, including the laser at 266 nm. This spectrum is used to determine the best fluorescence emission wavelength for the calibrations curve studies. This spectrum is in agreement with SO_2 spectra reported in the literature.[19]

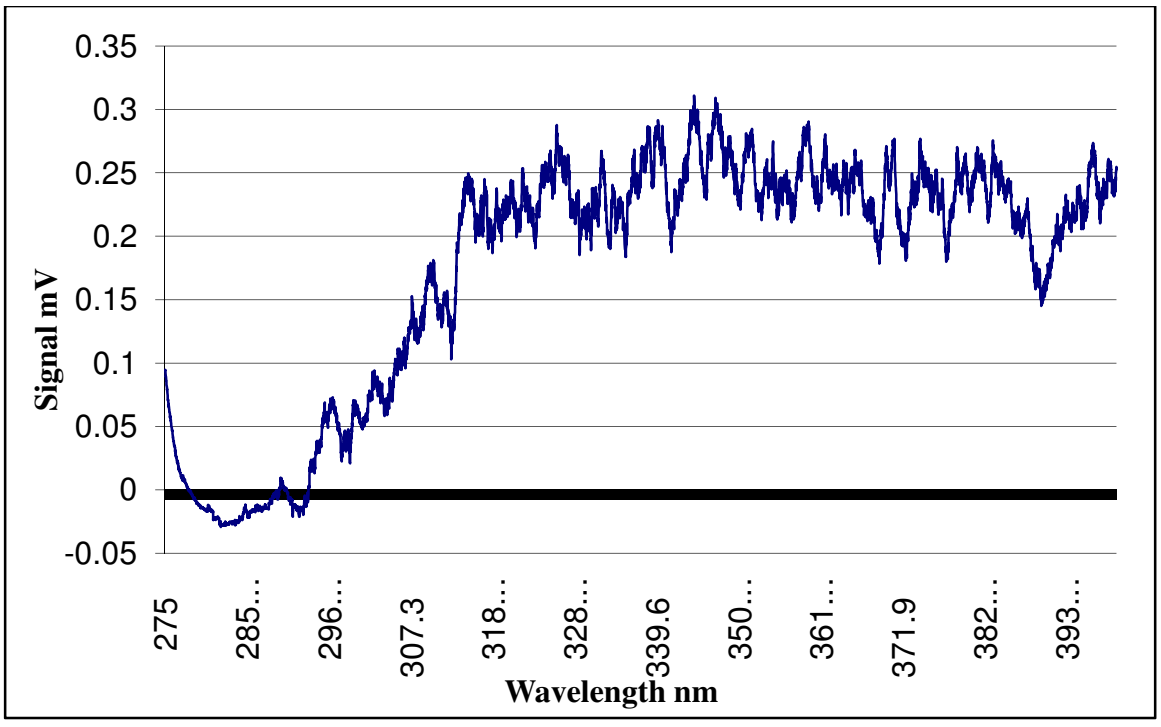

Figure (12) Spectrum of SO_2 from 275 nm - 400 nm with toluene filter

As the spectrum in figure 12 shows, fluorescence detection can be performed effectively over the 310 – 400 nm range.

b. <u>Power Dependence</u>:

Further measurements were conducted using a fluorescence detection wavelength of 360 nm. Power dependence studies were performed to evaluate the relationship of the fluorescence signal to the laser energy. The results of the power dependence studies for SO_2 are shown in figure (13) and indicate that the fluorescence response using laser excitation at 266 nm is not saturated, even at 8 mJ. This suggests that further increasing the laser pulse energy will increase the fluorescence signal. However, increases in the laser energy may also increase the background noise and the optimum signal to noise may occur at less than saturation values. These studies were also performed to determine the minimum energy that is required to produce a measurable signal. This helps to determine the feasibility of performing LIF measurements using a fiber optic for delivering the laser radiation, since high laser energies can damage the fiber optic.

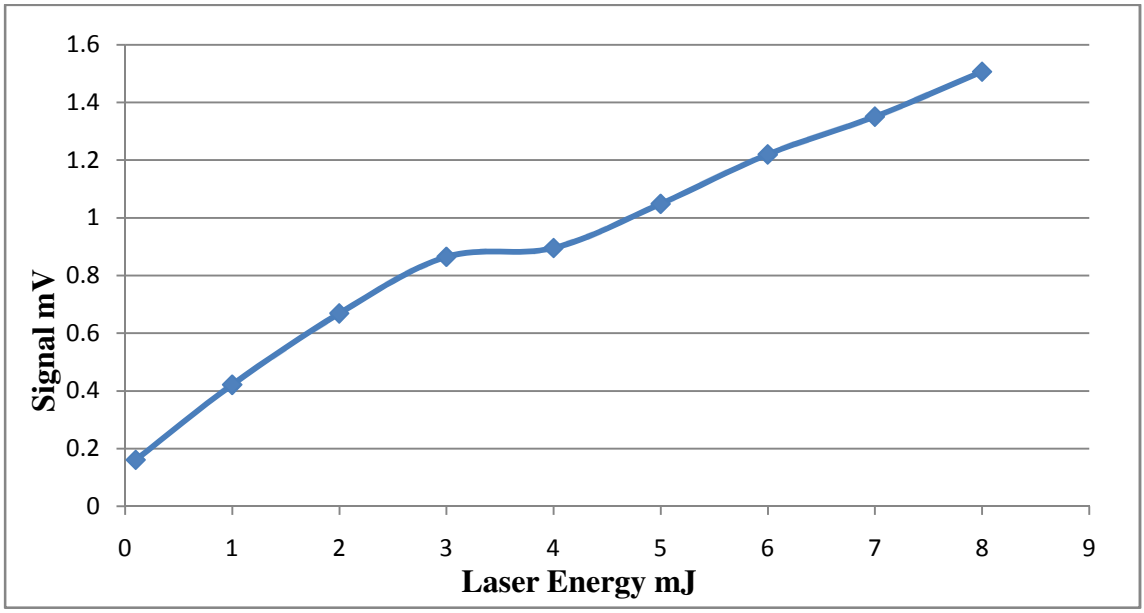

Figure: (13) Power dependence of SO_2 fluorescence with 266 nm laser excitation and fluorescence wavelength of 360 nm

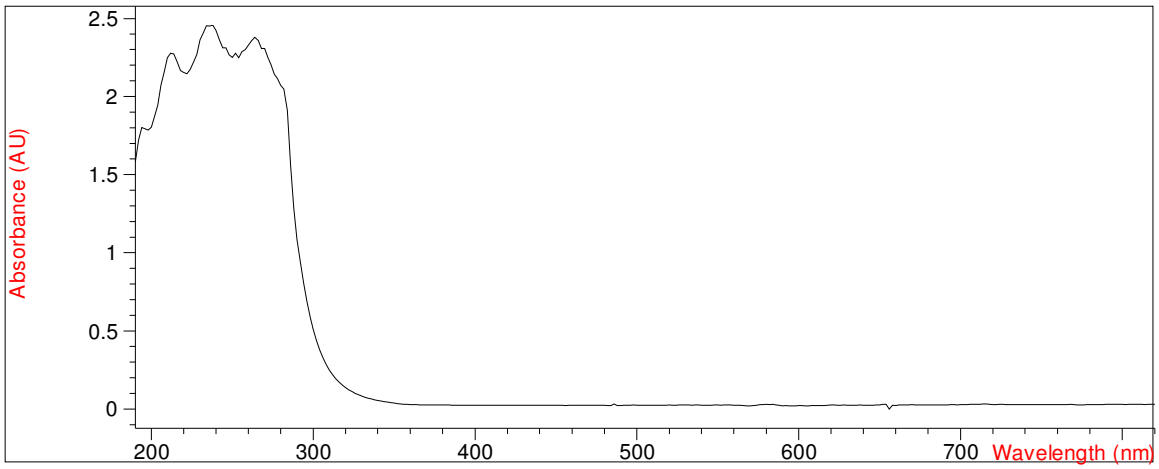

Figure: (14) Absorption Spectrum of Toluene filter

The absorption spectrum of the long pass toluene filter was acquired to determine filter properties. The absorption spectrum in figure (14) shows that the filter has significant absorption up to 300 nm and transmits efficiently beyond 300 nm. As the spectrum shows, the toluene filter is expected to block scattered laser radiation at 266 nm with high efficiency.

c. <u>Calibration Curve studies of SO_2 using 266 nm laser</u>:

Calibration curves were obtained using laser excitation at 266 nm and fluorescence detection at 360 nm. The slit widths of the monochromator were varied for different sets of data. Through these studies, it was possible to determine the best slit for LIF measurements. From the graph in figure (15) in which the calibration curves were done at different slits and at the same emission wavelength 360 nm, it was observed that the 3000 micron slit provided high sensitivity and a good detection limit. However the noise was also high, as is indicated by a lower R^2 value (0.9734). In order to improve the signal to noise ratio, a smaller slit (1000) was used. Calibration curves were also

performed at a fluorescence emission wavelength of 325 nm [shown in figure (16)] to determine which fluorescence wavelength provided a better LOD. The data indicate that the 360 nm provided better results.

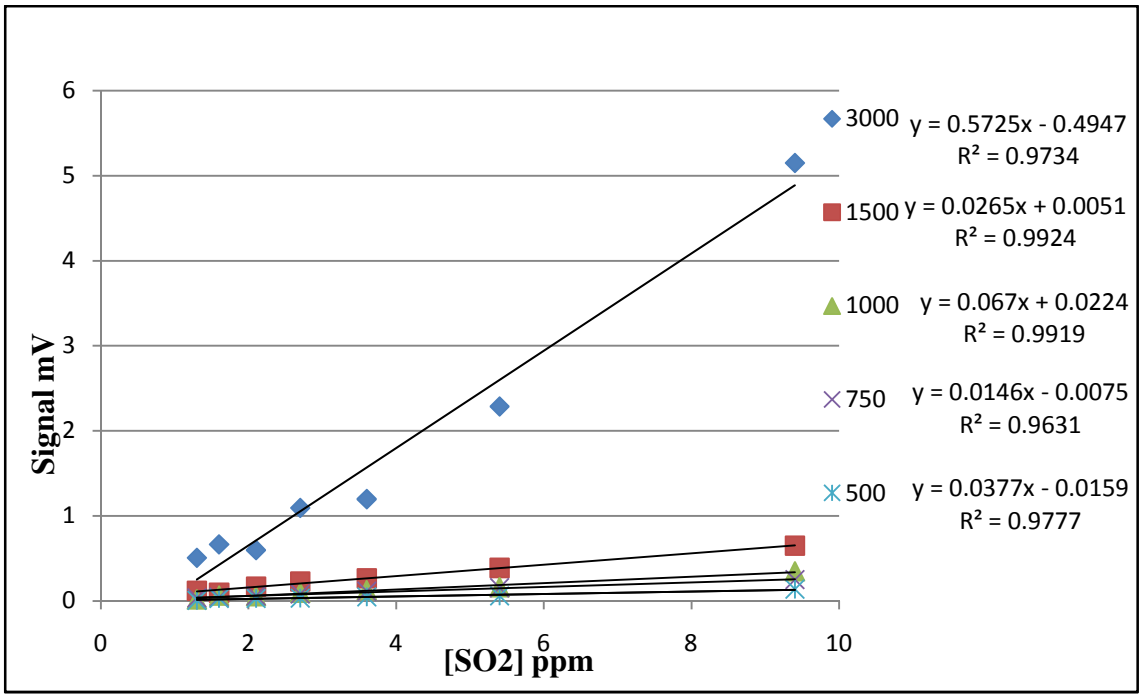

Figure: (15) Calibration curve of SO_2 fluorescence with 266 nm laser excitation at different slit widths

d. <u>Output scans of 266 nm from the Raman convertor</u>:

Excitation at 266 nm allows measurement of SO_2 at trace levels, however absorption data indicate that stronger SO_2 absorptions also occur at even lower wavelengths.[18] It may be possible to access some of these stronger absorptions by converting the Nd:YAG laser radiation by stimulated Raman scattering (SRS) to shorter wavelengths that coincide with SO_2 absorptions. The purpose of these studies was to evaluate these other wavelengths for LIF measurements of SO_2. The emission scan of the outputs from the Raman convertor filled with H_2 gas at 500 psi using a 266 nm laser is shown in Figure (17). The monochromator was scanned from 195 nm – 600 nm. The

spectrum shows nine wavelengths that are produced from Stokes and anti-stokes shifting. In these studies, the laser was converted to other wavelengths that were investigated for LIF measurements of SO_2. The spectrum shown in figure (17) is in agreement with SRS spectra reported previously for 266 nm excitation in H_2 gas.[26] Expected SRS outputs are predicted to occur at $\bar{V}_{output} = \bar{V}_{266} \pm n\ \bar{V}_{H2}$ where $\bar{V}$ =4155 cm^{-1}. Tables 3 and 4 list the expected SRS outputs for 266 nm and 355 nm laser radiation in H_2 gas.

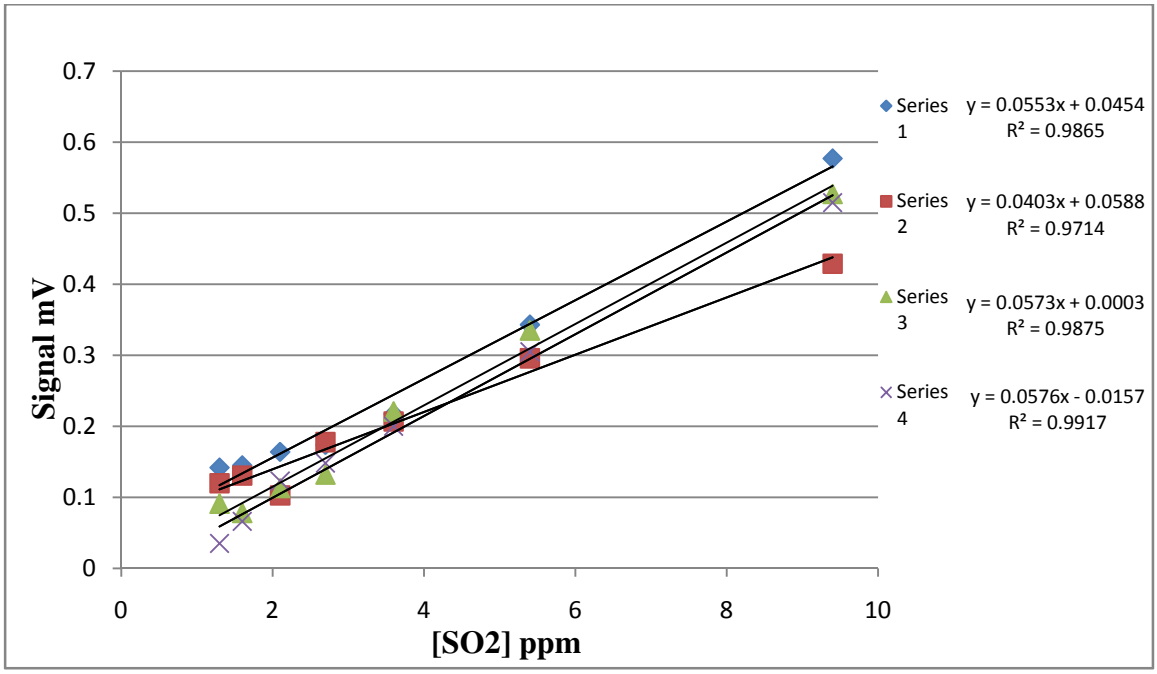

Figure: (16) Calibration curve of SO_2 fluorescence with 266 nm laser excitation and monochromator @ 325 nm

e. <u>Output scans of 355 nm from the Raman convertor</u>:

The scan of the outputs from the Raman convertor filled with H_2 gas at 500 psi using 355 nm laser is shown in Figure (18). The monochromator was scanned from 180 nm – 650 nm. The graph shows nine wavelengths that are produced from the Stokes and anti Stokes shifting. The spectrum is in agreement with SRS spectra reported previously

for 355 nm excitation in H_2 gas.[26] It is important to note that some of the less intense peaks in Figure (18) are second order transmissions of peaks, produced at ultraviolet wavelengths.

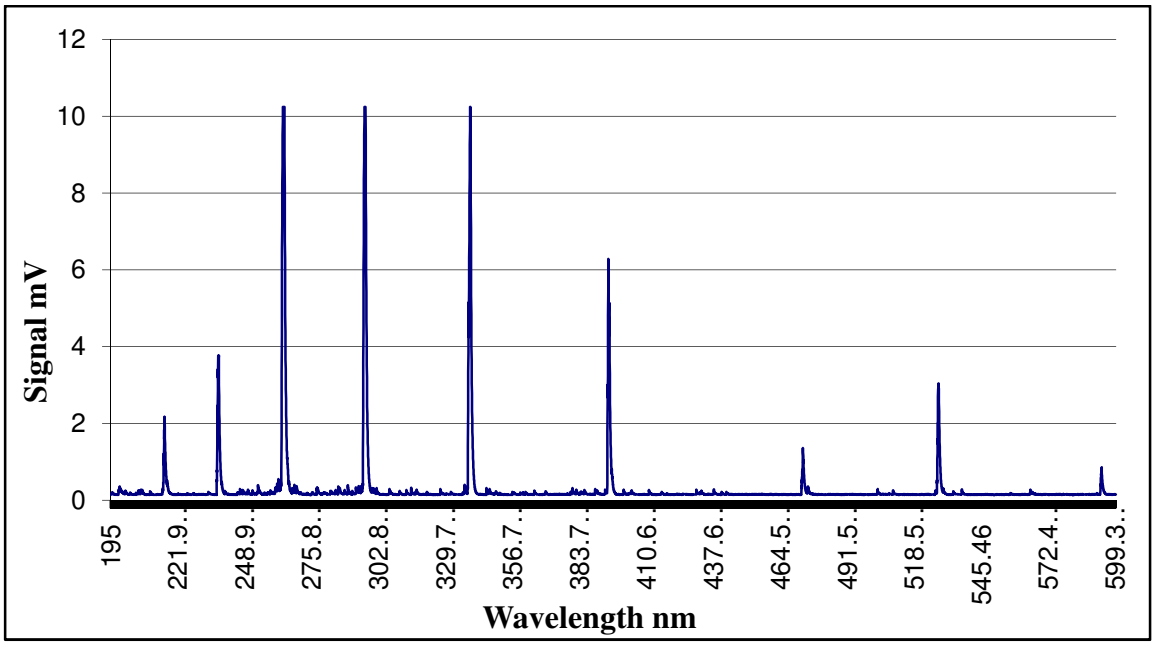

Figure: (17) Scan of the outputs of 266 nm laser through Raman convertor

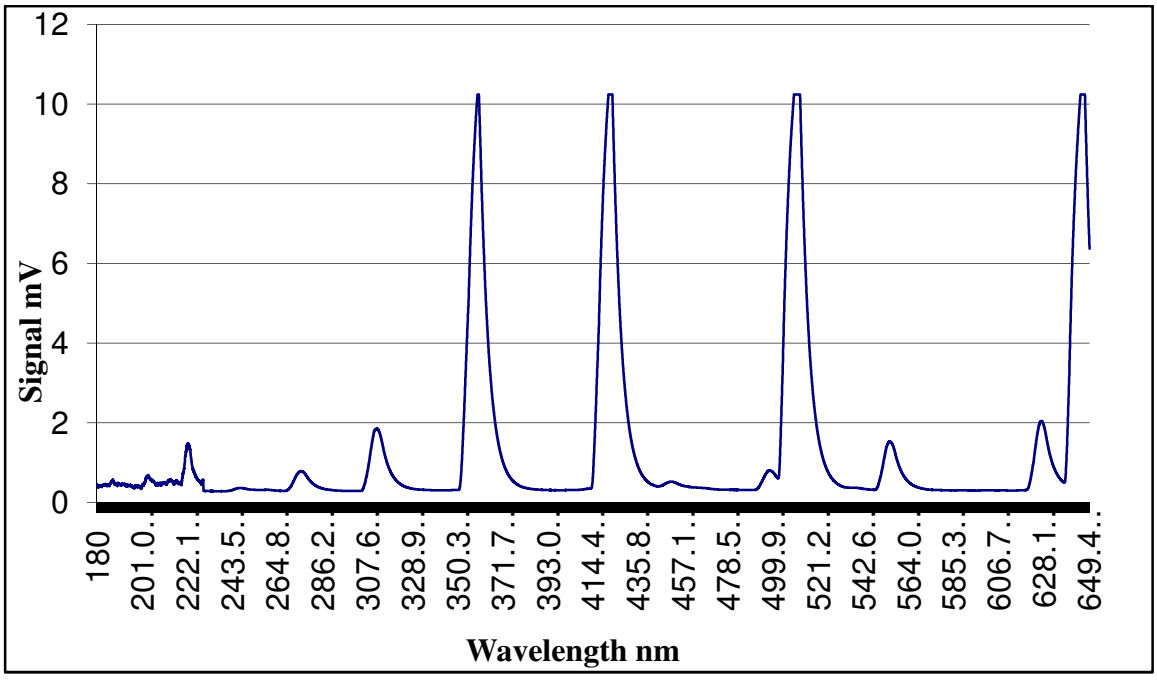

Figure: (18) Scan of the outputs of 355 nm laser through Raman convertor

It was of interest to determine the conversion efficiencies of each of the SRS outputs using 266 nm and 355 nm pumping. As shown in table (5) and table (6), each Raman shift is identified by its wavelength along with the measured energy at that wavelength. By measuring the total energy exiting the cell and the pulse energy at each output wavelength, it is possible to estimate the relative conversion efficiency for each output.

f. <u>Spectrum of SO_2 with 223 nm laser</u>:

Several wavelengths generated by the SRS shifts of 266 nm and 355 nm lasers are possible candidates for UV excitation of SO_2 fluorescence. A list of these wavelengths is shown in table (3) and table (4). One of the wavelengths investigated was at 223 nm. The spectrum of SO_2 fluorescence emission produced using 223 nm excitation was taken from 275 nm – 450 nm. Figure (19) shows the SO_2 fluorescence profile from 275 nm – 450 nm. There is a peak at 355 nm that is due to laser scatter by the 355 nm laser and a peak at 416 nm that is due to laser scatter by one of the outputs from the Raman convertor (table 4). Besides these signals, the SO_2 fluorescence spectrum using 223 nm excitation is observed to be similar to that produced using 266 nm excitation.

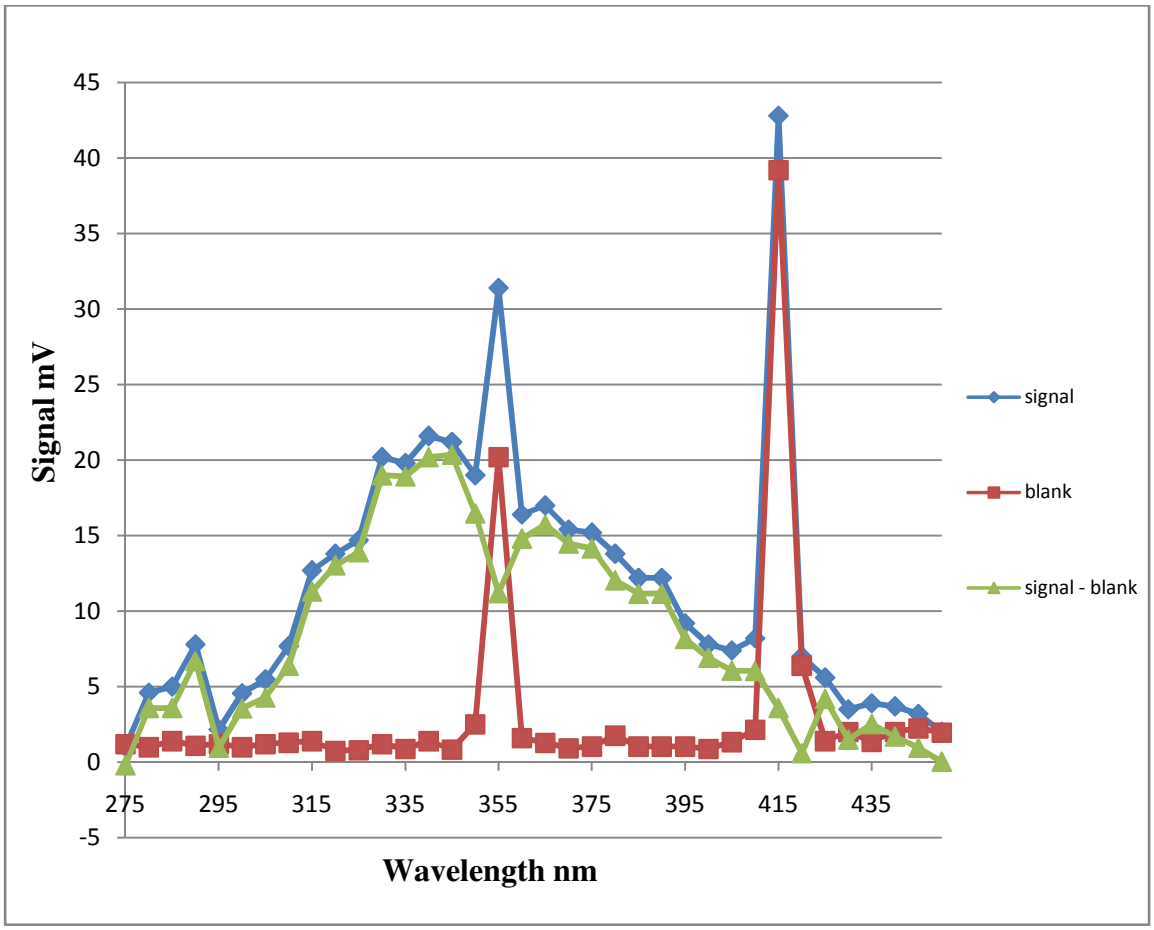

Figure: (19) Spectrum of SO_2 fluorescence with 223 nm laser excitation

S. No	Wavelength nm
5^{th} stokes	594.566
4^{th} stokes	476.78
3^{rd} stokes	397.9
2^{nd} stokes	341.48
1^{st} stokes	299
Fundamental	266
1^{st} anti stokes	239.5
2^{nd} anti stokes	217.85
3^{rd} anti stokes	199.76

Table: (3) Outputs of 226 nm laser through Raman convertor

S. No	Wavelength nm
5^{th} anti stokes	204.2
4^{th} anti stokes	223.2
3^{rd} anti stokes	246
2^{nd} anti stokes	274
1^{st} anti stokes	309.2
Fundamental	354.8
1^{st} stokes	416.2
2^{nd} stokes	503.2
3^{rd} stokes	636.2

Table: (4) Outputs of 355 nm laser through Raman convertor

g. Relative intensities:

Relative intensity of SRS outputs using 266 nm laser:

266 nm laser energy in front of the convertor – 11.6 mJ

Energy behind the convertor – 7.1 mJ

Wavelength nm	Energy mJ	Relative intensity
594.566	0.00013	0.013
476.78	0.008	0.11
397.9	0.105	1.5
341.48	0.256	3.6
299	0.167	2.4
266	0.231	3.3
239.5	0.033	0.5
217.58	0.013	0.2
199.76	0.001	0.01

Table: (5) Relative stimulated Raman scattering intensities of 266 nm laser

Relative intensity of SRS outputs using of 355 nm laser:

355 nm laser energy in front of the convertor – 18.0 mJ

Energy behind the convertor – 12.0 mJ

Wavelength nm	**Energy mJ**	**Relative intensity**
636.2	0.9	7.5
503.2	1.05	8.75
416.2	0.5	4.16
354.8	0.4	3.33
309	0.08	0.66
274	0.06	0.5
246	0.016	0.13
223.2	0.00224	0.02
204.2	0.000245	0.002

Table: (6) Relative stimulated Raman scattering intensities of 355 nm laser

h. <u>Trials with 199 nm and 217 nm laser</u>:

Attempts were made to excite SO_2 fluorescence at other wavelengths such as 199 nm and 217 nm. As the literature data indicate, SO_2 shows strong absorption bands near these wavelengths.[28, 29] In fact, lamp – based fluorescence measurements are performed using Zn lamp excitation near 213 nm.[8] Attempts to measure SO_2 fluorescence using these other ultraviolet excitation wavelengths did not yield good results. This could be due to the fact that SO_2 undergoes photodissociation at wavelengths below 220 nm.

$$SO_2 \xrightarrow[h\nu]{} SO_2^* \quad (9)$$

$$SO_2^* \longrightarrow SO_2 + h\nu \quad (10)$$

$$SO_2 \longrightarrow SO + O \quad (11)$$

According to previous studies, the rate of non radiative decays including photodissociation increases significantly at wavelengths below 220 nm and these decays are able to compete effectively with fluorescence emission.[30] The wavelengths 199 nm and 217 nm excite the SO_2 molecule beyond the threshold leading to photodissociation. At these wavelengths, the SO_2 molecule is taking up this energy and breaking apart due to which there is no fluorescence given.[31] As a result, it is not unexpected that no significant fluorescence was observed in these studies when 199 nm or 217 nm excitation were used. It is worth noting, however, that commercial lamp–based fluorescence systems use excitation at 213 nm for SO_2 measurements.[8]

The power dependence of SO_2 using the 223 nm laser shown in figure (20) showed possible saturation, which indicates that much less energy may be required to excite the SO_2 to give the maximum fluorescence response as compared to excitation at 266 nm. This is in agreement with the stronger absorption band at 223 nm compared to 266 nm.

Based on the reported absorbance data for SO_2 in these wavelength regions, it is expected that the laser excitation rate may be as much as 200 times greater at 223 nm compared to excitation at 266 nm due to higher transmission probability.

i. <u>Calibration curve studies of 223 nm laser</u>:

Calibration curve studies were performed to find the best limit of detection of SO_2 by LIF using 223 nm laser excitation. Shown in figure (21) are calibration curve data obtained using the stainless steel cell and a monochromator. As seen, the fourth trial gave the lowest LOD of all the trials which corresponds to a LOD value of 0.3 ppm.

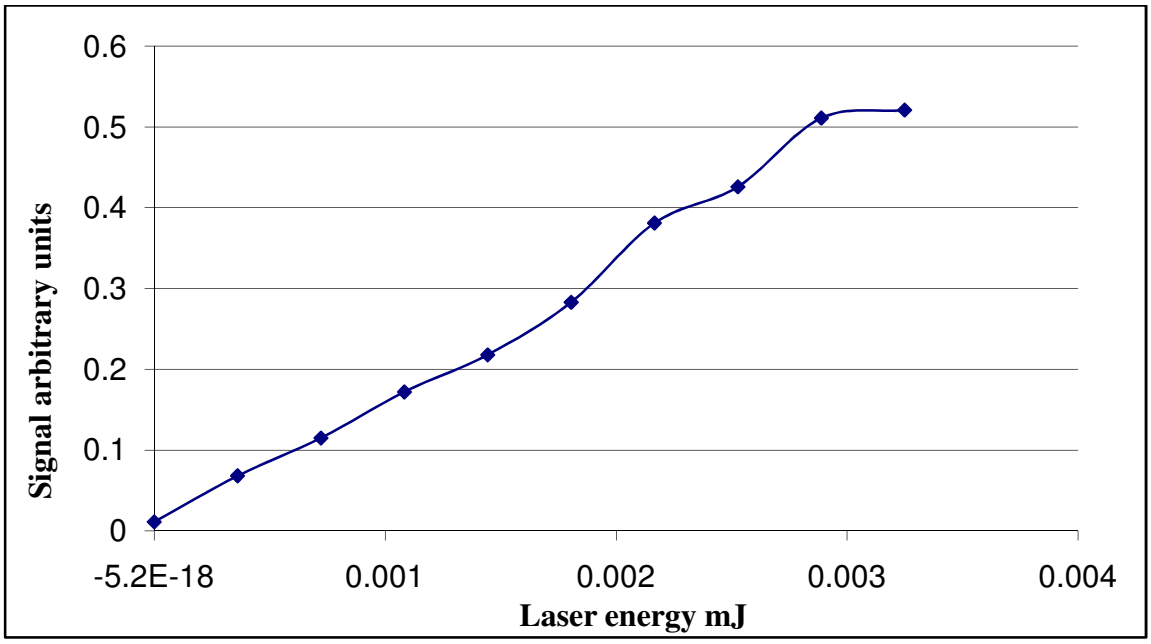

Figure: (20) Power Dependence of SO_2 fluorescence with 223 nm laser excitation and closed sample cell and monochromator

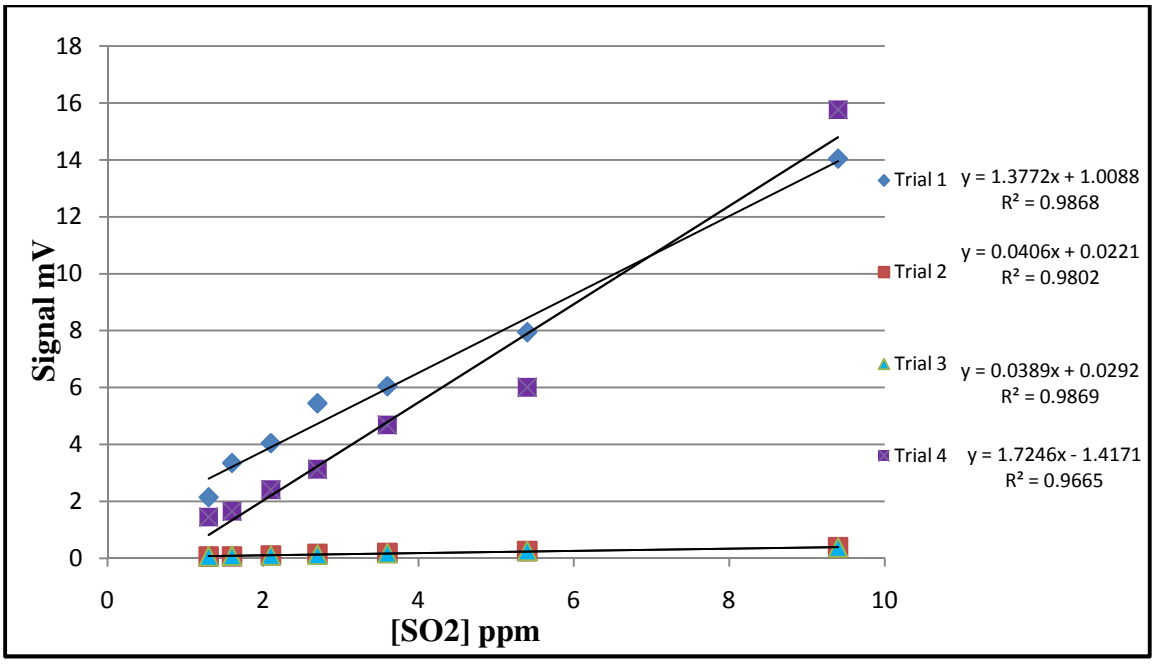

Figure: (21) Calibration Curve of SO_2 fluorescence with 223 nm laser excitation, closed sample cell and monochromator

The 223 nm laser was relatively low in intensity and diverged as it traveled towards the sample cell. For this reason, a cylindrical focusing lens was used to focus the beam in the form of a horizontal stripe in the sample cell. This was expected to increase the laser intensity so that a large area of strong fluorescence could be detected in the cell and possibly increase the sensitivity. Shown in figure (23) is a graph of 3 trials of calibration curves using a cylindrical focusing lens. Trial three had the lowest LOD which corresponds to a value of 0.099 ppm.

To increase the sensitivity further, the monochromator was replaced with a PMT (photomultiplier tube) and filter (334 nm band pass filter) having a band pass of 10 nm where emissions near 334 nm are allowed and the rest of the light is blocked with high efficiency. While the monochromator collects a small spectral window of the fluorescence emission at the set wavelength, the band pass filter allows a larger emission

band of 10 nm from a larger spatial area into the detector. This allows the SO_2 fluorescence to be collected over a wide range of wavelengths and also from a larger volume. Both of these factors are expected to improve the sensitivity and the LOD. The absorption spectrum of the 334 nm band pass filter is shown in figure (22) which shows high absorbance up to about 320 nm and then high transmission nearly up to 340 nm. This shows that the filter transmits a band of wavelength in between 330 nm and 340 nm.

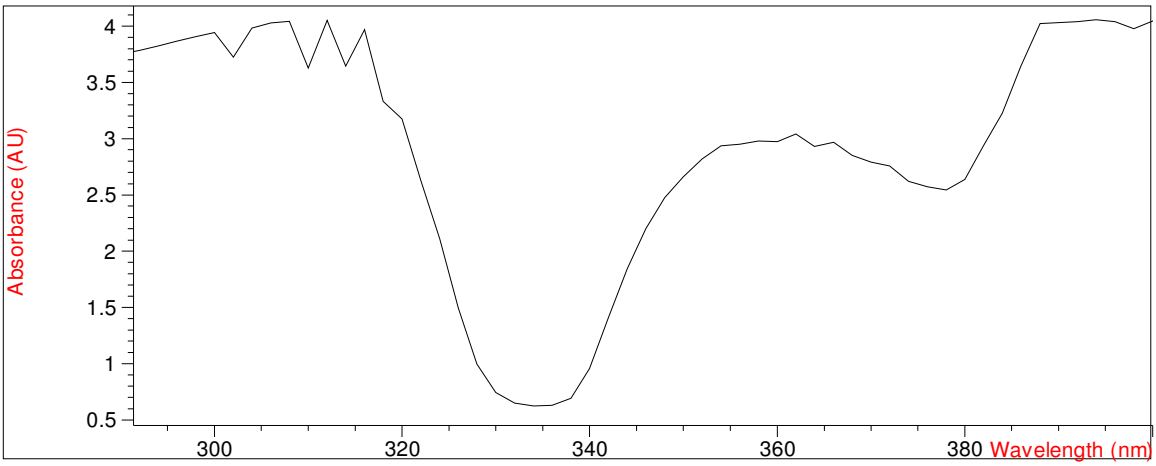

Figure: (22) Absorption Spectrum of the 334 nm band pass filter

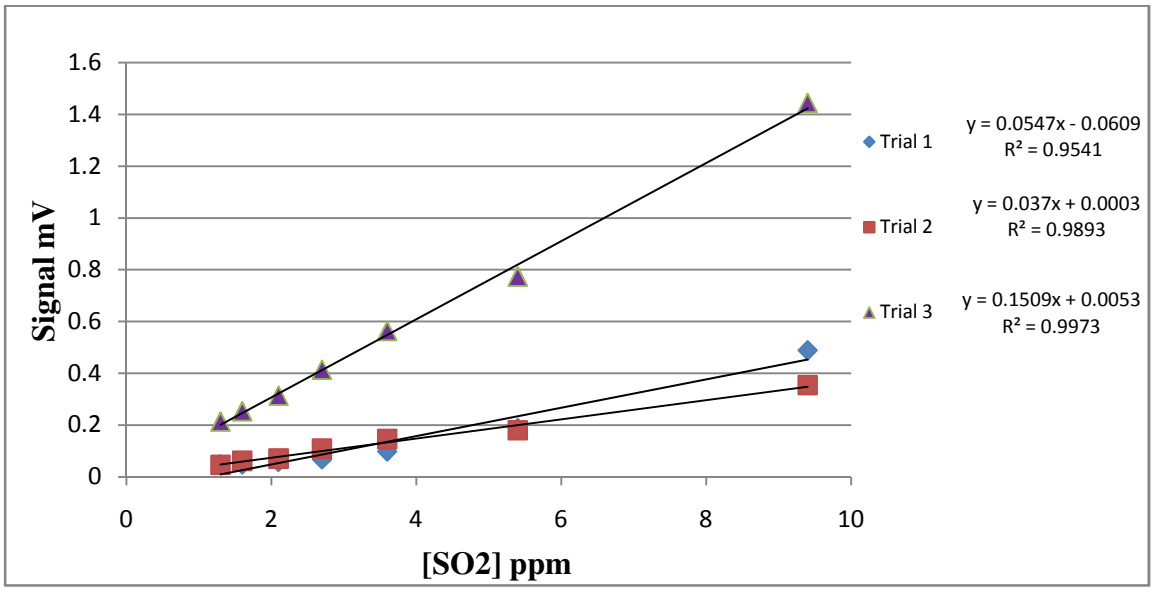

Figure: (23) Calibration curve of SO_2 fluorescence with 223 nm laser excitation, closed sample cell, cylindrical focusing lens and PMT/filter

While the use of a cylindrical focusing lens and the PMT/filter combination helped to improve the LOD, a spherical focusing lens was also used with the same set of conditions to see if this would further improve the results. This focusing lens focuses the beam to a point where the intensity of the laser beam is increased. Figure (24) shows the results of calibration curves obtained using a focusing lens, the closed steel sample cell and a PMT/filter combination. In these studies, the temperature of the permeation tube device was also varied from 50 ^{0}C to 40 ^{0}C. Both calibration curves are shown together in figure (24). The LOD at 50 ^{0}C was 0.026 ppm and for 40 ^{0}C the LOD was 0.025 ppm. These results indicate that the focusing lens helps to improve the LOD by increasing the laser intensity in the detection volume.

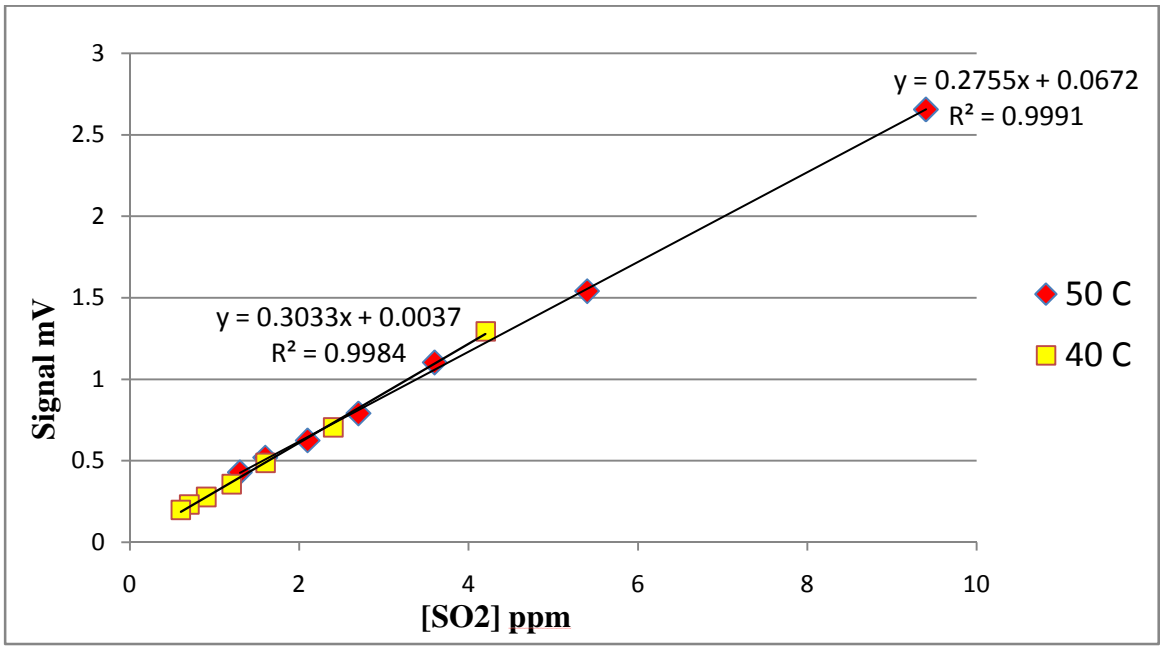

Figure: (24) Calibration of SO_2 fluorescence with 223 nm laser excitation, T-cell and @ different temperatures

To simplify the arrangement and reduce the background noise, an alternative sample cell was used. As the closed stainless steel sample cell has windows, it produces a significant background due to reflections and scatter of the laser from the cell windows. An alternative "T" – cell was used that has no windows on both sides so the laser is able to pass through without reflecting off windows and as a result provides a lower background.

A calibration curve was performed with the T – cell and monochromator at different slit widths. The figure (25) shows the calibration curve at 1000 and 3000 micron slit widths and the LOD was almost the same for both the calibration curves. The calibration curve with 3000 slit provided the lowest LOD (0.09 ppm) obtained in this graph.

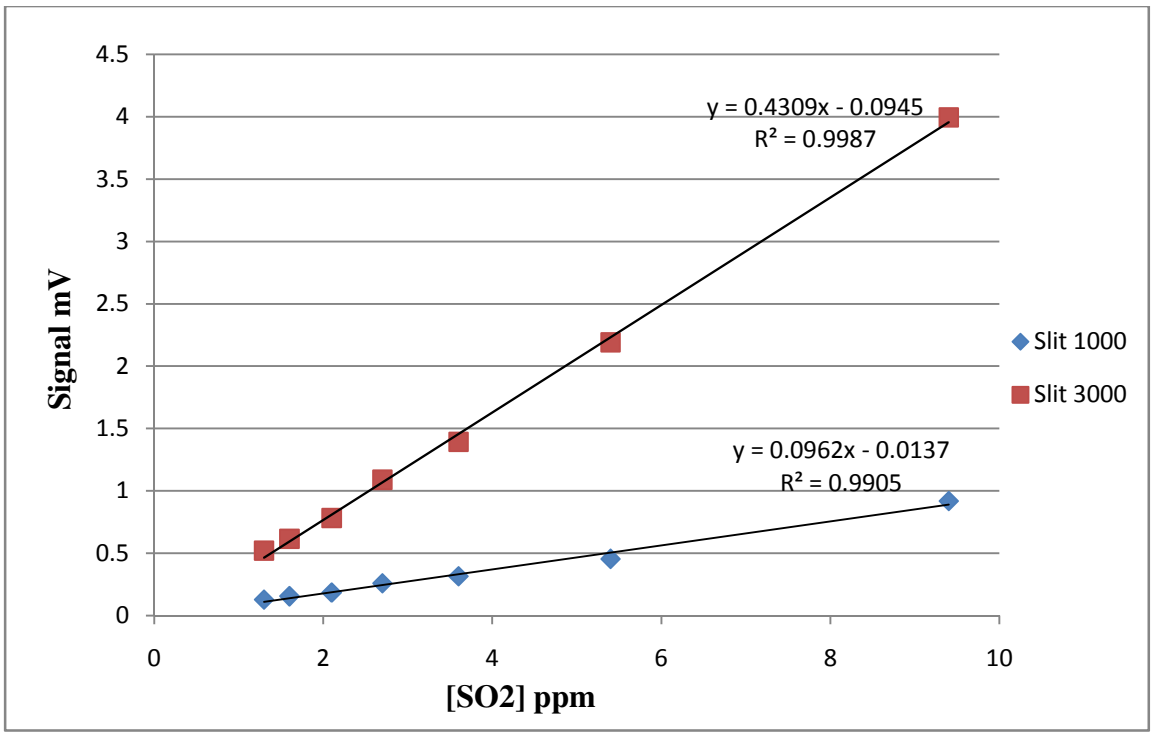

Figure: (25) Calibration curve of SO_2 fluorescence with 223 nm laser excitation, T-cell and @ different slit widths

The power dependence studies were done with the T – cell and monochromator combination to check the saturation of the fluorescence signal. However, the LIF signal does not show any saturation as is shown in figure (27). A similar study was performed for power dependence for the T – cell, PMT and filter combination and these results are shown in figure (28).

The lowest LOD was 10 ppb obtained from the T – cell, PMT/filter and focusing lens combination and the temperature of the permeation tube was maintained at 40 ^{0}C. These data are shown in figure (26).

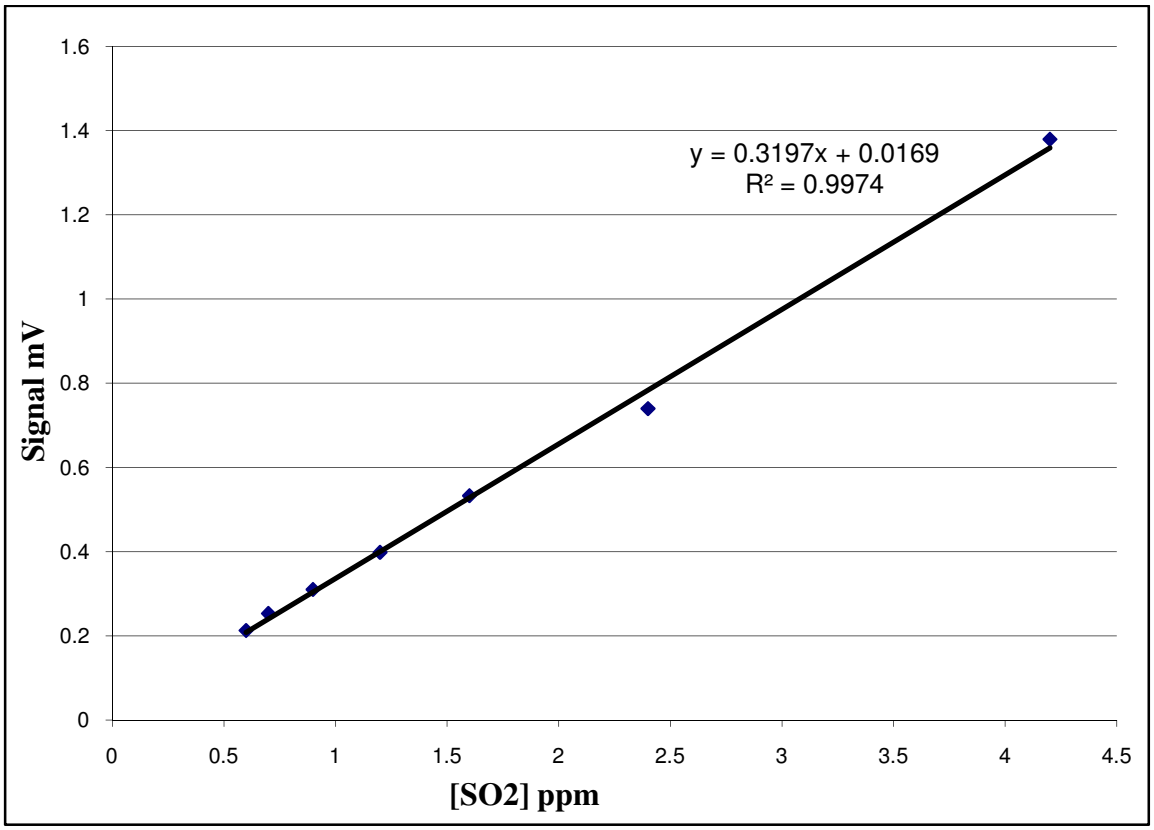

Figure: (26) Calibration curve of SO_2 fluorescence with 223 nm laser excitation @ temp-40 ^{0}C, with PMT filter, T-cell and focusing lens.

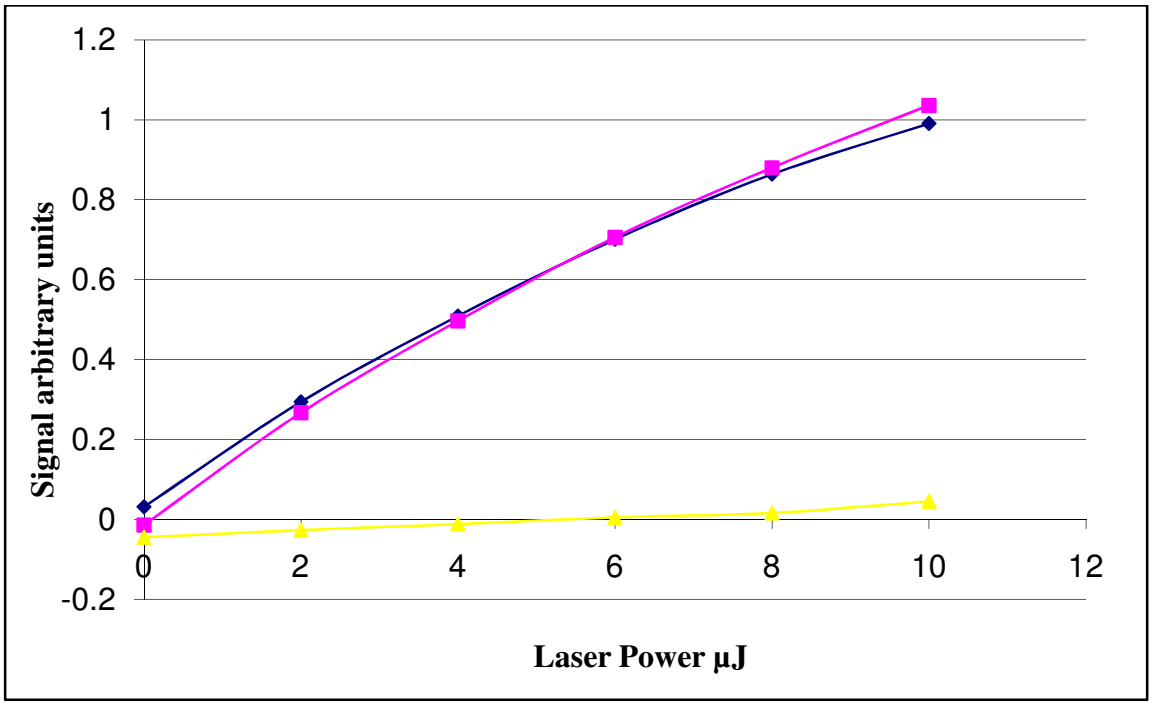

Figure: (27) Power Dependence of SO_2 fluorescence with 223 nm laser excitation, T-cell and monochromator

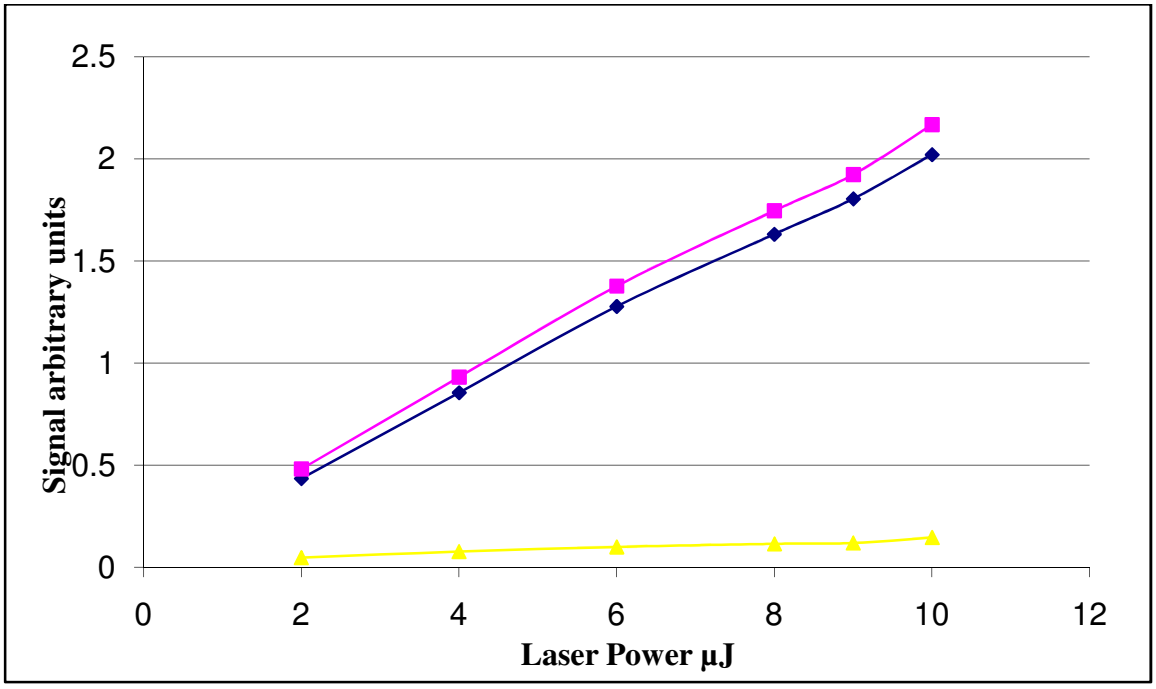

Figure: (28) Power Dependence of SO_2 fluorescence with 223 nm laser excitation, T-cell and PMT/filter

j. Comparison of results of 266 nm and 223 nm:

The signal in the case of 223 nm excitation was large when compared to 266 nm and also the background was much less when compared to 266 nm. It is also worth noting that the laser energy was much less for 223 nm laser than at 266 nm.

The fluorescence intensity depends on the lifetime of the excited state. The shorter the fluorescence lifetime, the higher will be the fluorescence intensity. According to Bradshaw et al., the C ($^1B_2$) state, has a much shorter lifetime compared to the B ($^1B_1$) state. [18] The lifetimes are approximately 45 vs. 50 μsec for the first excitation state.[18]

$$SO_2X\ (^1A_1) + h\nu_1 \xrightarrow[(\lambda_1 = 222\ nm)]{} SO_2\ C\ (^1B_2)\ [\alpha_1\ (0, 2)\ transition] \quad (12)$$

$$SO_2\ C\ (^1B_2) \xrightarrow[(\lambda_2 = 230 - 320\ nm)]{} SO_2X\ (^1A_1) + h\nu_2 \quad (13)$$

As a result, the fluorescence intensity may be expected to be lower using 266 nm excitation compared to 223 nm excitation based on the fluorescence lifetimes. This is consistent with the results of these studies which show that 223 nm excitation leads to higher fluorescence and higher sensitivity than excitation at 266 nm.

k. Comparison of signal and background for 266 nm and 223 nm:

Laser wavelength	Laser Energy mJ	Signal mV	Background mV
266 nm	0.5 mJ	2.06 mV	1.42 mV
223 nm	0.003 mJ	2.45 mV	0.167 mV

Table: (7) Comparison of signal and background for 266 nm and 223 nm laser excitation

From the data in table (7) it can be concluded that the fluorescence given out in the case of 223 nm excitation wavelength is 200 times higher when compared to 266 nm laser

excitation wavelength. The laser energies that used are approximately 300 times less in the case of 223 nm laser excitation. The background is also much less in the case of 223 nm laser excitation wavelength. So it was expected that the 223 nm laser excitation wavelength gives better LODs.

l. <u>Interference studies of formaldehyde (HCHO)</u>:

The possible interference of formaldehyde (HCHO) on the fluorescence of SO_2 was studied. In order to evaluate this, the fluorescence spectrum of a HCHO/air mixture was taken with the 223 nm laser, which is the laser wavelength used for the excitation of SO_2. The spectrum shown in figure (29) indicates that there is no significant fluorescence signal from HCHO. From this it can be expected that HCHO will not interfere in the fluorescence measurement of SO_2 when 233 nm laser excitation is used. This was also demonstrated through the calibration curve in figure (30). As seen in figure (30), there is very weak correlation between fluorescence intensity and the concentration of HCHO using excitation at 223 nm.

If the data are assumed to be linearly correlated, then the data suggests that HCHO may produce a weak interference signal that is approximately 22 times lower than that of SO_2.

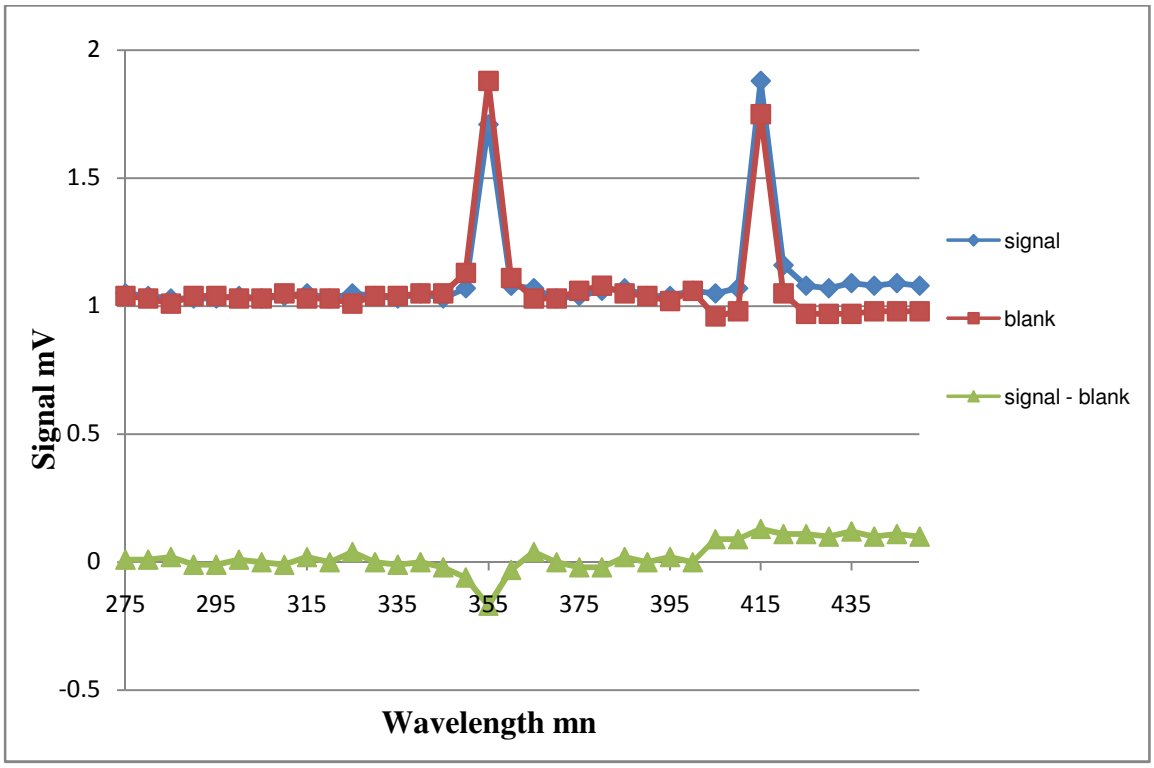

Figure: (29) Spectrum of HCHO fluorescence with 223 nm laser excitation, for interference studies

m. <u>Other Interferences</u>:

Water vapor is reported to have a quenching effect on the fluorescence signal. It has been reported that a 20% ± 10% quenching of the signal was observed with 50% relative humidity. [7] The presence of 16 g m^{-3} H_2O will quench the fluorescence by 10%. [9, 8] In order to get the precise measurement in the presence of water vapor, it is better to take two different measurements, one for SO_2 and the other for H_2O. For other gases to interfere, the concentration of those gases reportedly need to be nearly 100 times higher than SO_2.[8] The concentration of NO and NO_2 should be 1000 times more than SO_2.[9]

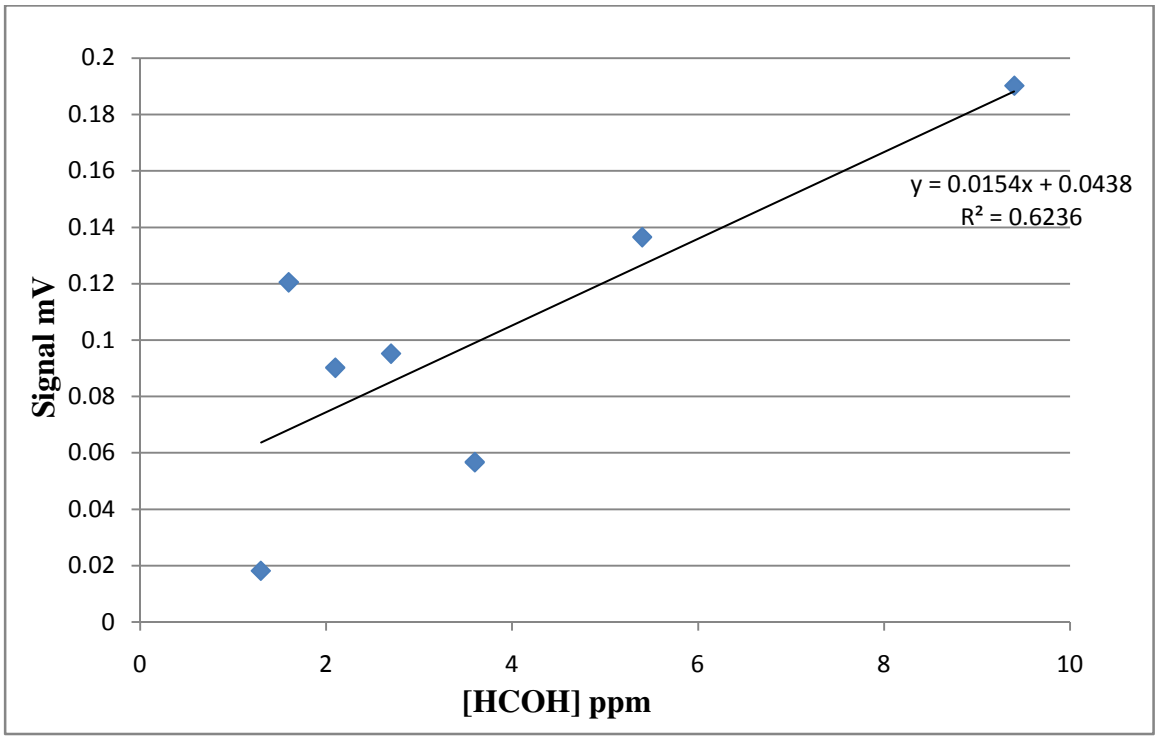

Figure: (30) Calibration curve of HCHO fluorescence with 223 nm laser excitation for interference studies

It is interesting to compare the results obtained here using a non-tunable laser source for LIF measurements of SO_2 with those reported previously. Shown in table (8) are the reported limits of detection for various methods used for SO_2 detection in air which includes LIF results in references [9] and [18] that are the lowest shown.

It should be noted that the LIF results in these studies were obtained using non-tunable lasers, whereas the other LIF results were obtained using tunable laser sources where the laser output wavelengths were matched with the peak of the absorption band at 222 nm. It should also be noted that there are significant differences in the laser energies used. In this work, relatively small pulse energies are used that are approximately 300 times smaller than what was used in the other cases. Considering that LIF intensity is linearly related to the source intensity when the laser excitation is not saturated, this

n. <u>Comparison of LOD with other work</u>:

Method used	LOD (ppb)	Integration time	Sample type	Laser energy mJ	Reference
LIF with 266 nm	393	1.30 min	No alteration	0.231 mJ	this work
LIF with 223 nm	10	1.30 min	No alteration	0.003 mJ	this work
LIF with 222.2 nm (Dye laser)	0.005	1 min	No alteration	1 mJ	[19]
Single photon LIF 222 nm	0.0016	20 min	H_2O from air is removed	1 mJ	[18]
Fluorescence with Zn 213.8 nm & Cd 228.8 nm lamps	20	1 min	No alteration	NA	[8]
Fluorescence with Zn 213.8 nm	8.6-1.8	5 min	Dry air was used	NA	[9]
Diode laser UV absorption spectroscopy	2000	0.87 min	Dry air was used	NA	[32]
Gas Chromatography	50	NA	Separation of SO_2	NA	[33]
H_2 flame Spectrophotometry	100-1300	NA	Purified grade Hydrogen fuel was used as no response could be seen with room air	NA	[34]

Table: (8) Comparison of Limit of Detection of this work with other studies

factor alone accounts for almost the entire difference in the detection capability in terms of the LODs. This is expected that higher laser energies, higher repetition rates and higher signal averaging could also be used to increase the sensitivity and lower the LOD for this approach.

o. <u>Conclusions</u>:

The results obtained to this point demonstrate that trace concentrations of SO_2 can be detected by a direct LIF approach using non tunable lasers. The power dependence studies indicate that the signal is proportional to the laser energy suggesting that increases in laser energy may further increase the measurement capabilities. The current detection limits of 10 ppb for SO_2 is good and is expected to be improved.

p. <u>Further studies</u>:

In future studies, optical fibers are to be used to deliver the laser light from the source to the sample cell so that there is better efficiency in the delivering of laser energy to the sample cell. The interference studies of HCHO should be investigated further to determine the actual interference potential of this compound. The use of a larger opening T – cell should be investigated to study the improvement of the LODs. It is also of interest to study the 266 nm laser with the T – cell, PMT and filter combination. It is also of interest to evaluate another emission wavelength for the 223 nm laser excitation. Studies on the fluorescence quenching due to water should be done and finally the use of methane as the Raman medium and also the mixture of methane and hydrogen as a Raman medium should be studied.

4. REFERENCES

1. West, P. W.; Gaeke, G. C. *Anal. Chem.* **1956***, 28*, 1816-1819.

2. Smith, S. J.; Pitcher, H.; Wigley, T. M. L. *Clim. Change* **2005***, 73*, 267-318.

3. Komarnisky, L. A.; Christopherson, R. J.; Basu, T. K. *Nutrition* **2003***, 19*, 54-61.

4. Zh, Z.; Río, A.; Valcárce, M. *Analyst* **1995***, 120*, 2013-2018

5. Bradshaw, M. P.; Scollary, G. R.; Prenzler, P. D. *J. Sci. Food Agric.* **2004***, 84*, 318-324

6. Stevens, R. K.; O'Keeffe, A. E.; Ortman, G. C. *Environ. Sci. Technol.* **1969***, 3*, 652-655.

7. Schwarz, F. P.; Okabe, H.; Whittaker, J. K. *Anal. Chem.* **1974***, 46*, 1024-1028.

8. Okabe, H.; Splitstone, P. L.; Ball, J. J. *J. Air Pollut. Control Assoc.* **1973***, 23*, 514.

9. Jaeschke, W.; Beltz, N. Haunold, W. *Journal of Geophysical Research, [Atmospheres]* **1997***, 102*, 16279.

10. Luke, W. T. *Journal of Geophysical Research, [Atmospheres]* **1997***, 102*, 16255.

11. Bandy, A. R.; Thornton, D.C.; Driedger III, A. R. *Journal of Geophysical Research, [Atmospheres]* **1993***, 98*, 23423.

12. Talbot, R. W.; Scheuer, E. M.; Lefer, B. L. *Journal of Geophysical Research, [Atmospheres]* **1997***, 102*, 16273.

13. Benner, R. L.; Thornton, D. C.; Driedger III, A. R. *Journal of Geophysical Research, [Atmospheres]* **1997***, 102*, 16287.

14. Gallagher, M. S.; King, D. B.; Saltzman, E. S. *Journal of Geophysical Research, [Atmospheres]* **1997***, 102*, 16247.

15. Ferek, R. J.; Covert, P. A.; Luke, W. *Journal of Geophysical Research, [Atmospheres]* **1997***, 102*, 16267.

16. Thornton, D. C.; Brandy, A. R.; Tu, F. H. *Journal of Geophysical Research* **2002***, 107*, ACH13.

17. Platt, U.; Perner, D. *Journal of Geophysical Research, C: Oceans and Atmospheres* **1980***, 85*, 7453.

18. Bradshaw, J. D.; Rodgers, M. O.; Davis, D. D. *Appl. Opt.* **1982***, 21*, 2493.

19. Matsumi, Y.; Shigemori, H.; Takahashi, K. *Atmos. Environ.* **2005***, 39*, 3177-3185.

20. Sune Svanberg In *Atomic and Molecular Spectroscopy Basic Aspects and Practical Applications;* Arthur L. Schawlow and Koichi Shimoda, Ed.; Springer- Verlag: 1990; pp 132.

21. Rufus, J.; Stark, G.; Smith, P. L.; Pickering, J. C.; Thorne, A. P. *Journal of Geophysical Research* **2003***, 108*, 5.

22. Sick, V. *Applied Physics B Lasers and Optics* **2002***, 74*, 461-463.

23. Muller, C. H.,III *Symp Int Combust* **1979***, 17*, 867.

24. Washenfelder, R. A.; Roehl, C. M.; McKinney, K. A.; Julian, R. R.; Wennberg, P. O. *Rev. Sci. Instrum.* **2003***, 74*, 3151-3154.

25. Bruno, T. J. *Journal of Chromatography A* **1995***, 704*, 157-162.

26. Jarvis, G. B. *Appl. Opt.* **1994***, 33*, 4938.

27. Sune Svanberg In *Atomic and Molecular Spectroscopy Basic Aspects and Practical Applications;* Arthur L. Schawlow and Koichi Shimoda, Ed.; Springer- Verlag: 1990; , pp 122.

28. Ahmed, S. M.; Vijay, K. *Journal of Quantitative Spectroscopy and Radiative Transfer* **1992***, 47*, 359.

29. Manatt, S. L.; Lane, A. L. *Journal of Quantitative Spectroscopy and Radiative Transfer* **1993***, 50*, 267.

30. Okabe, H. *J. Am. Chem. Soc.* **1971***, 93*, 7095-7096.

31. Hui, M. H,; Rice, S. A. *Chemical Physics Letters* **1972***, 17*, 474.

32. Somesfalean, G.; Zhang, Z. G.; Sjoholm, M.; Svanberg, S. *Applied Physics B* **2005***, 80*, 1021-1025.

33. Stevens, R. K.; Mulik, J. D.; O'Keeffe, A. E.; Krost, K. J. *Anal. Chem.* **1971***, 43*, 827-831.

34. Crider, W. L. *Anal. Chem.* **1965***, 37*, 1770-1773.

35. Klein, R.M. *Photochem. Photobiol.* **1979***, 29*, 1053.